International Journal of
Plant Biology

MDPI

Article

Foliar Nanoparticles Improve Growth, Photosynthetic Performance, and Mineral Nutrition in Field-Grown Jalapeño Pepper Under Severe Water Limitation

Erick H. Ochoa-Chaparro [1], Sandra Pérez-Álvarez [2] and Esteban Sánchez [1,*]

[1] Unidad Delicias, Centro de Investigación en Alimentación y Desarrollo (CIAD), Av. Cuarta Sur 3828, Fracc. Vencedores del Desierto, Delicias C.P. 33089, Chihuahua, Mexico; eriicktronik@hotmail.com
[2] Facultad de Ciencias Agrícolas y Forestales, Universidad Autónoma de Chihuahua (UACH), Km 2.5 Carretera a Rosales, Delicias C.P. 33000, Chihuahua, Mexico; spalvarez@uach.mx
* Correspondence: esteban@ciad.mx; Tel.: +639-549-46-81

Abstract

Severe water limitation constrains crop productivity through coordinated effects on growth, photosynthetic performance, and mineral nutrition. This study evaluated whether foliar nanoparticle (NP)-based formulations and commercial biostimulants could improve the physiological and productive performance of field-grown jalapeño pepper (*Capsicum annuum* L.) receiving 50% of the reference irrigation volume. Treatments included ZnO NPs, SiO_2 NPs, ZnO + SiO_2 NPs, Nano ZnMo, Osmoplant, and Codasil, together with well-watered and water-limited controls. Severe water limitation markedly reduced stem and fruit biomass, aboveground biomass, and fruit yield, despite relatively stable instantaneous gas exchange. Foliar treatments induced distinct responses. ZnO NPs produced the strongest productive recovery, restoring fruit dry biomass to well-watered levels and increasing fruit yield by 72.8% relative to the water-limited control. Codasil maximized net photosynthesis, photochemical quenching, and electron transport rate, whereas Osmoplant produced the highest water-use and intrinsic water-use efficiencies. ZnO + SiO_2 NPs maximized carboxylation efficiency, while Nano ZnMo partially restored Fe and maintained a distinctive mineral profile. Correlation and principal component analysis (PCA) showed that productivity was primarily associated with coordinated gas exchange and photochemical traits. Finally, the ZnO NP-based formulation showed the greatest improvement in fruit yield among the evaluated foliar treatments under water-limited conditions, highlighting its potential for sustaining jalapeño pepper productivity.

Keywords: *Capsicum annuum* L.; fruit yield; gas exchange; nanoparticles; photosynthesis; water-use efficiency; ZnO NPs

Check for updates

Academic Editor: Cheng Chang

Received: 11 September 2026
Revised: 26 October 2026
Accepted: 28 October 2026
Published: 30 October 2026

Copyright: © 2026 by the authors. Licensee MDPI, Basel, Switzerland. This article is an open access article distributed under the terms and conditions of the Creative Commons Attribution (CC BY) license.

1. Introduction

Plant growth is one of the physiological processes most sensitive to water deficit, as reduced water availability restricts cellular and tissue expansion [1], decreases shoot growth, alters root system architecture [2], limits biomass accumulation, and reduces crop yield [3]. In horticultural species, water deficit stress also disrupts coordination among morphological, physiological, biochemical, and molecular processes required to sustain vegetative and reproductive development, potentially compromising crop establishment, growth, and yield [4]. In jalapeño pepper (*Capsicum annuum* L.), restricted water availability causes morphological alterations, including reduced leaf area, restricted growth, and

lower biomass accumulation, ultimately resulting in decreased yield. It also affects photosynthetic processes by reducing gas exchange and transpiration due to stomatal closure. These alterations may induce oxidative damage and impair photosynthetic efficiency, which can be assessed through chlorophyll fluorescence measurements [5]. These simultaneous responses indicate that growth inhibition under water deficit cannot be attributed to a single physiological limitation but rather results from the disruption of the coordinated processes that supply carbon, water, and mineral nutrients to developing organs. Therefore, identifying foliar strategies to improve growth and productivity under limited water availability is particularly relevant to the sustainable production of jalapeño pepper in semiarid agricultural regions.

The ability of plants to sustain growth under water deficit largely depends on maintaining photosynthetic activity, as carbon assimilation is the primary source of photoassimilates required for biomass accumulation [6]. One of the earliest physiological responses to water deficit is stomatal closure, a mechanism that reduces transpirational water loss but also restricts CO_2 diffusion into the leaf mesophyll and progressively decreases the net photosynthetic rate [7]. As water limitation intensifies, reduced carbon fixation generates an imbalance between absorbed light energy and its utilization in the Calvin cycle, increasing the risk of photoinhibition and oxidative damage to the photosynthetic apparatus [8]. Consequently, the ability to maintain photosystem II photochemical efficiency and electron transport represents an essential physiological component for sustaining plant growth and productivity under conditions of limited water availability [9].

The maintenance of plant growth and photosynthetic performance under limited water availability also depends on adequate mineral nutrition, as several mineral elements participate in stomatal regulation, photochemical energy conversion, electron transport, and antioxidant defense. Reduced soil water content restricts nutrient diffusion and mass flow toward the rhizosphere, thereby decreasing nutrient uptake and transport within the plant. As a consequence of water deficit, the uptake and concentrations of several mineral nutrients, including phosphorus, potassium, calcium, and magnesium, may decline, disrupting mineral nutrition and further constraining plant growth [10]. Likewise, micronutrients such as iron, manganese, zinc, and copper act as cofactors or structural components of proteins involved in redox processes, photosynthetic reactions, and antioxidant defense systems and therefore play essential roles in maintaining plant metabolism and growth [11,12]. Thus, maintaining an adequate mineral nutrient balance is important for sustaining physiological functioning and plant growth when water availability is restricted [10].

In response to the effects of water deficit, foliar-applied nanoparticles have emerged as an innovative strategy to improve crop growth and productivity due to their ability to simultaneously modulate physiological, biochemical, and metabolic processes associated with stress adaptation [13]. Among them, zinc oxide nanoparticles (ZnO NPs) have been shown to enhance photosynthetic activity, promote biomass accumulation, and strengthen antioxidant systems, thereby contributing to greater performance under limited water availability [14]. Foliar application of ZnO NPs has also been reported to improve the accumulation of compatible osmolytes and the uptake of mineral nutrients, favoring the maintenance of plant growth under limited water availability [15]. Similarly, silicon dioxide nanoparticles (SiO_2 NPs) help maintain plant water status, stomatal regulation, and photosynthetic efficiency while reducing oxidative damage associated with restricted water availability [16]. Moreover, incorporating biocompatible polymers such as chitosan into nanoparticle-based formulations may improve their stability and contribute to plant responses under limited water availability. In common bean, foliar application of chitosan nanoparticles improved yield and several physiological and biochemical attributes under drought conditions [17]. Despite recent advances, much of the available knowledge regard-

ing the use of nanoparticles to enhance tolerance to water deficit has been derived from experiments conducted under controlled conditions. Therefore, field studies integrating growth, photosynthesis, mineral nutrition, and productivity under severe water limitation are still needed [18].

Therefore, the objective of this study was to determine whether foliar applications of ZnO and SiO_2 nanoparticles, their combined formulation, a ZnMo nanofertilizer, and commercial biostimulants promote growth and productivity in field-grown jalapeño pepper (*Capsicum annuum* L.) under severe water limitation through coordinated changes in photosynthetic performance and mineral nutrition. To address this objective, gas exchange, PSII photochemical performance, chlorophyll status, biochemical responses, mineral nutrient composition, biomass accumulation, and fruit yield were evaluated in an integrated manner. We hypothesized that nanoparticle-based formulations and biostimulants would mitigate the effects of severe water limitation by sustaining photosynthetic carbon assimilation, PSII photochemical performance, and mineral nutrient balance, thereby promoting biomass accumulation and fruit yield.

2. Materials and Methods

2.1. Plant Material and Growth Conditions

The experiment was conducted during the spring–summer 2025 growing season at the experimental field of the Faculty of Agricultural and Forestry Sciences, Autonomous University of Chihuahua (UACH), located in Delicias, Chihuahua, Mexico (28.655204° N, 106.087289° W; 1170 m a.s.l.). Jalapeño pepper plants (*Capsicum annuum* L. cv. Imperial F1) were used. Seedlings were produced under greenhouse conditions (12–33 °C and 30–45% relative humidity) under a natural photoperiod in 200-cell polystyrene trays (2 × 2 × 5 cm) filled with a 1:1:1 (*v*/*v*/*v*) mixture of vermiculite, perlite, and Sphagnum peat moss (Premier® Sphagnum Peat Moss, Rivière-du-Loup, QC, Canada). After 60 days of growth, when the seedlings reached the commercial transplanting stage, uniform plants were selected and transplanted to the field on 1 April 2025, with a spacing of 0.35 m between plants and 0.60 m between rows.

Throughout the crop cycle, all plants received the same agronomic management, including fertigation and weed, pest, and disease control, according to standard commercial practices for jalapeño pepper production. The final destructive harvest was performed on 11 August 2025.

2.2. Soil Characteristics

Before transplanting, composite soil samples were collected from the surface layer (0–30 cm depth) and analyzed at a certified laboratory (Fertilab, Celaya, Guanajuato, Mexico). Based on particle-size distribution, the experimental soil was classified as loam. The initial physical properties of the soil are presented in Table 1, while the main chemical properties and concentrations of available macro- and micronutrients are shown in Table 2.

Table 1. Initial physical properties of the experimental soil.

Layer (cm)	Texture (Class)	Bulk Density (g cm^{-3})	Ksat (cm h^{-1})	FC (%)	WP (%)
0–30	Loam	1.33	2.95	18.0	10.7

Table 2. Initial chemical properties of the experimental soil.

Properties	Value
pH (soil:water ratio 1:2)	7.78
ECe (dS m^{-1}; saturated paste extract)	3.28
CEC (cmolc kg^{-1})	23.2
$CaCO_3$ (%)	8.13
Organic matter (%)	3.67
Exchangeable sodium percentage (ESP, %)	9.66
Available nutrients:	
Nutrient (mg kg^{-1} soil)	**Value**
$N\text{-}NO_3$	47.3
P-Olsen	44.2
K	372
Ca	3587
Mg	253
Fe	4.51
Mn	11.4
Zn	5.41
Cu	1.90
B	2.44
S	252

ECe = electrical conductivity of the saturated paste extract; CEC = cation exchange capacity; ESP = exchangeable sodium percentage.

2.3. Irrigation Program and Imposition of Water Limitation

Irrigation was supplied through a drip irrigation system using drip tape with pressure-compensating emitters spaced 0.35 m apart. The volume of water applied during each irrigation event was calculated from the nominal emitter flow rate and the system operating time, according to Equation (1):

$$V_{total} = \sum_{i=1}^{n} (Q_i \, x \, t_i) \quad (1)$$

where V_{total} is the total volume of water applied per plant throughout the crop cycle (L $plant^{-1}$), (Q_i) corresponds to the nominal emitter flow rate at each phenological stage (L h^{-1} $plant^{-1}$), (t_i) represents the irrigation system operating time for each irrigation event (h), and (n) is the total number of irrigation events.

The irrigation schedule was adjusted according to the crop phenological stage. During establishment and vegetative growth (0–22 days after transplanting, DAT), emitters with a flow rate of 1.0 L h^{-1} $plant^{-1}$ were used. During flowering (23–45 DAT), the flow rate was increased to 1.5 L h^{-1} $plant^{-1}$. During fruit development (46–66 DAT) and the harvest period (67–132 DAT), emitters with a flow rate of 2.0 L h^{-1} $plant^{-1}$ were used.

A total of 43 irrigation events were carried out throughout the crop cycle. Irrigation scheduling was based on the estimated crop evapotranspiration (ETc), with the reference irrigation schedule corresponding to an approximate cumulative volume of 134 L $plant^{-1}$ over the entire crop cycle. Plants in the well-watered control (Control-WW) received 100% of the estimated crop irrigation requirement, whereas plants in the water-limited control (Control-WL) and those subjected to the six foliar treatments received 50% of this requirement, equivalent to approximately 67 L $plant^{-1}$. Water limitation was imposed by reducing the volume of water applied while maintaining the same irrigation frequency throughout the experiment [19,20].

Irrigation frequency, application schedule, and all other agronomic management practices were identical across treatments; only the volume of water applied differed by irrigation regime. The distribution of irrigation events across the different phenological stages is presented in Table 3.

Table 3. Irrigation management during the crop cycle.

Growth Stage	Duration (Days)	Irrigation Events
Establishment and vegetative growth	22	8
Flowering	23	8
Fruit development	21	7
Harvest period	66	20

2.4. Fertigation Program

Crop mineral nutrition was supplied through fertigation using NutriNet® software v. 2025 [21], which was used to design and adjust the nutritional program to meet crop requirements at different phenological stages. Fully water-soluble fertilizers (GreenHow®, Guadalajara, Mexico) were used, including calcium nitrate, phosphonitrate, monopotassium phosphate (MKP), potassium nitrate, and magnesium sulfate as macronutrient sources, while micronutrients were supplied as Fe-EDDHA, manganese sulfate, Solubor® (B), and copper sulfate.

Nutrient solutions were prepared in separate tanks to avoid chemical incompatibilities among fertilizers and were subsequently injected into the irrigation system during each fertigation event. The nutritional program was adjusted as crop development progressed, with the supply of phosphorus, potassium, and magnesium progressively increased during the fruiting stages to meet the greater nutrient demand associated with fruit growth and filling, while the supply of calcium and nitrogen was maintained according to the physiological requirements of the crop.

The nutrient solution had a pH of 6.0 ± 0.1 and an electrical conductivity (EC) of 1.57–1.60 mS cm^{-1} throughout the crop cycle. Fertigation was managed independently of the irrigation regimes to ensure equivalent nutrient inputs per plant across all treatments. During each irrigation event, fertilizer-free water was initially supplied, followed by the application of the nutrient solution at the same concentration, flow rate, and duration for both irrigation regimes. Differences in irrigation volume were subsequently established by adjusting the duration of fertilizer-free water application. Thus, all treatments received equivalent nutrient inputs, whereas the cumulative irrigation volumes differed between the well-watered (134 L $plant^{-1}$) and water-limited (67 L $plant^{-1}$) regimes.

2.5. Characterization of Nanoparticles and Commercial Biostimulants

The zinc oxide nanoparticles (ZnO NPs) and silicon dioxide nanoparticles (SiO_2 NPs) used in this study were supplied by Investigación y Desarrollo de Nanomateriales S.A. de C.V. (San Luis Potosí, Mexico). The physicochemical characterization provided by the manufacturer included scanning electron microscopy (SEM), transmission electron microscopy (TEM), energy-dispersive X-ray spectroscopy (EDX), and X-ray diffraction (XRD) analyses for ZnO NPs. For SiO_2 NPs, the available characterization consisted of manufacturer-provided TEM micrographs. The characterization results provided by the manufacturer are described in Section 3.1.

In addition to the nanoparticle-based formulations, three commercial products were included as comparative treatments: Nano ZnMo (Agrichem Fluagri, Guadalajara, Jalisco, Mexico), Osmoplant (BioIbérica, Barcelona, Spain), and Codasil (Atlántica Agrícola, Alicante, Spain). According to the manufacturers' technical datasheets, Nano ZnMo contains

62% zinc, 5% molybdenum, and 5% chelating agents derived from seaweed extracts; Osmoplant contains 6% free amino acids, 2.4% nitrogen, and 3.3% potassium; and Codasil is a soluble silicon-based formulation containing 20% silicon, 4% free amino acids, and 11.2% potassium. Independent physicochemical characterization of the commercial Nano ZnMo formulation was not available for this study, and its reported composition was taken from the product datasheet.

2.6. Experimental Design and Treatments

The experiment was conducted under field conditions using a conventional drip irrigation system comprising four experimental rows. Two rows were randomly assigned to the well-watered regime (100% of the reference irrigation volume), whereas the remaining two rows were assigned to the water-limited regime (50%). Irrigation was supplied through a central valve connected to individual control valves installed in each row, allowing independent time-based regulation of water application at the row level. The well-watered control (Control-WW) was established in the two rows receiving 100% irrigation, whereas the water-limited control (Control-WL) and the six foliar treatments were randomly distributed within the two rows receiving 50% irrigation. A total of 96 plants were established, comprising 12 plants per treatment, with six plants allocated to each corresponding row. Three plants were randomly selected from each row, resulting in six evaluated plants per treatment and 48 sampled plants. Individual plants served as the units of foliar treatment application and biological sampling, whereas the irrigation rows represented the experimental units for irrigation management, with two independently regulated rows per irrigation regime. Plant spacing was 0.35 m within rows and 0.60 m between rows.

The treatments consisted of a well-watered control (Control-WW), which received 100% of the reference irrigation volume; a water-limited control (Control-WL), which received 50% of the reference irrigation volume; and six foliar treatments subjected to the same 50% irrigation regime: ZnO NPs, SiO_2 NPs, ZnO + SiO_2 NPs, Nano ZnMo, Osmoplant, and Codasil. The composition and application rates of the foliar formulations are presented in Table 4.

Table 4. Composition, application rates, and irrigation regimes of the treatments evaluated injalapeño pepper.

Treatment	Foliar Formulation	Application Rate	Irrigation Regime
Control-WW	No foliar application	Not applicable	100%
Control-WL	No foliar application	Not applicable	50%
ZnO NPs	ZnO NPs + chitosan	100 mg L^{-1} + 100 mg L^{-1}	50%
SiO_2 NPs	SiO_2 NPs + chitosan	10 mg L^{-1} + 100 mg L^{-1} Ch	50%
ZnO + SiO_2 NPs	ZnO + SiO_2 NPs + chitosan	100 mg L^{-1} + 10 mg L^{-1} + 100 mg L^{-1}	50%
Nano ZnMo	Zn + Mo	124 mg Zn L^{-1} + 10 mg Mo L^{-1}	50%
Osmoplant	Commercial biostimulant	2 mL L^{-1}	50%
Codasil	Silicon-based commercial biostimulant	2 mL L^{-1}	50%

WW, well-watered; WL, water limitation; Ch, chitosan. Irrigation regimes correspond to the percentage of the reference irrigation volume (100% = 134 L $plant^{-1}$; 50% = 67 L $plant^{-1}$) applied throughout the crop cycle. For brevity, the treatment labels ZnO NPs, SiO_2 NPs, and ZnO + SiO_2 NPs used throughout the manuscript refer to the corresponding nanoparticle formulations containing chitosan. All application rates refer to the concentrations of the respective components in the prepared foliar solutions.

Six randomly selected plants per treatment were used for biomass, fruit yield, SPAD, gas exchange, and chlorophyll fluorescence assessments ($n = 6$). Subsequently, three of these six plants were randomly selected for biochemical and mineral analyses ($n = 3$), considering the available laboratory resources. Each selected plant represented an individual

biological sampling unit for the corresponding measurements. All six foliar treatments were applied five times at seven-day intervals, on 11, 18, and 25 April and 2 and 9 May 2025, using a previously calibrated manual backpack sprayer. The composition of the commercial formulations, including their Zn, Mo, Si, K, and amino acid contents, is described in Section 2.5, whereas the application concentrations of each treatment are presented in Table 4. Approximately 1200 mL of foliar solution was applied per treatment at each application, equivalent to approximately 108 mL plant^{-1}. Over the five foliar applications, each treatment received a cumulative volume of 3.25 L. Applications were performed to ensure uniform foliar coverage while minimizing spray drift between treatments.

Foliar solutions were prepared using distilled water as the solvent and a commercial water-soluble chitosan (poly-D-glucosamine) as a stabilizing and dispersing agent in nanoparticle-containing formulations. Before each application, the nanoparticle-containing solutions were homogenized by magnetic stirring for 60 min, followed by sonication for 15 min, to promote adequate nanoparticle dispersion. Magnetic stirring and sonication were used to promote nanoparticle dispersion before foliar application. However, particle size distribution, aggregation, and suspension stability were not directly evaluated in this study.

2.7. Plant Sampling

Plant sampling was conducted at 132 days after transplanting (DAT), at the end of the crop cycle and after completion of the commercial harvests. Six randomly selected plants per treatment were destructively harvested and separated into leaves, stems, and fruits for biomass determination ($n = 6$). Due to laboratory resource limitations, three of these six plants were randomly selected for biochemical and mineral analyses ($n = 3$). The same three plants were used for all biochemical and mineral determinations, ensuring consistency across the analytical measurements. Each sampled plant represented an independent biological observation for the corresponding analyses.

2.8. Plant Analysis

2.8.1. Biomass and Yield Determination

Fresh biomass was determined at the final destructive harvest in leaves, stems, and fruits from six plants per treatment using an analytical balance (HR-120, A&D Company Ltd., San Jose, CA, USA). For dry biomass determination, the same six plants from each treatment were separated by organ (leaves, stems, and fruits), individually placed in paper bags, and dried in a forced-air oven (Shell Lab Forced Air Laboratory Oven SMO14-108 2, Baltimore, MD, USA) at 70 °C for 72 h until constant weight was reached [22]. Dry biomass was subsequently recorded for each organ. Fresh and dry biomass were expressed as g plant^{-1} on a fresh-weight (FW) and dry-weight (DW) basis, respectively.

Fruit yield was determined from the cumulative fresh weight of fruits harvested from the same six plants per treatment during three commercial harvests conducted at 73, 98, and 130 days after transplanting (13 June, 8 July, and 9 August 2025, respectively). Fruits were harvested when they reached the commercial maturity stage characteristic of the cultivar. Cumulative fruit yield was expressed as g plant^{-1}.

2.8.2. Chlorophyll Index (SPAD)

Leaf chlorophyll status was estimated at 60 days after transplanting (DAT) using a portable chlorophyll meter (SPAD-502, Konica Minolta Sensing Inc., Osaka, Japan), a non-destructive method widely used to estimate the relative chlorophyll content of plant leaves [23]. Measurements were performed on five fully expanded, healthy leaves from each of six independent plants per treatment ($n = 6$), avoiding the central midrib and any visibly damaged or senescent tissue. For each leaf, a single reading was taken at the

central portion of the lamina, and the average of the five leaf readings was considered one experimental observation per plant and expressed in SPAD units.

2.8.3. Photosynthetic Gas Exchange, Water-Use Efficiency, and Fluorescence

Leaf gas exchange was evaluated at 45 DAT, during the reproductive stage of the crop, using a portable LI-6400XT photosynthesis system (LI-COR Biosciences, Lincoln, NE, USA) equipped with OPEN software v.4.06. Measurements were conducted between 11:00 and 15:00 h on fully expanded, healthy, and physiologically active leaves from six plants per treatment ($n = 6$), once the measured variables had stabilized within the leaf chamber [24].

The leaf chamber was configured under controlled conditions with a photosynthetic photon flux density (PPFD) of 1000 µmol m^{-2} s^{-1}, a reference CO_2 concentration of 410 µmol mol^{-1}, a block temperature of 25 °C, a target relative humidity of 70%, and a fan speed of 10,000 rpm, to ensure uniform conditions throughout all measurements.

The gas exchange variables recorded were net CO_2 assimilation rate (P_N), stomatal conductance (gs), transpiration rate (E), intercellular CO_2 concentration (Ci) and leaf vapor pressure deficit (VpdL). From these variables, water-use efficiency (WUE = P_N/E), intrinsic water-use efficiency (WUEi = P_N/gs), and carboxylation efficiency (CE = P_N/Ci) were calculated. These indices integrate the relationships among carbon assimilation, stomatal regulation, and transpirational water loss and are therefore widely used as indicators of plant physiological performance and adaptation to water deficit [7,25,26].

Chlorophyll fluorescence measurements were performed simultaneously using an LI-6400-40 fluorescence chamber coupled to the LI-6400XT system, with actinic light containing a 6% blue-light fraction. Measurements were conducted on light-adapted leaves without prior dark adaptation, under a photosynthetic photon flux density (PPFD) of 1000 µmol m^{-2} s^{-1}. The maximum efficiency of photosystem II in light-adapted leaves (Fv′/Fm′), photochemical quenching coefficient (qP), and electron transport rate (ETR) were determined. These parameters provide information on the photochemical performance of photosystem II under the evaluated conditions [8,9].

2.8.4. Photosynthetic Pigments

Photosynthetic pigments were extracted and quantified according to the method described by Wellburn [27]. Ten leaf discs (7 mm diameter) were collected from fully expanded, healthy, and photosynthetically active leaves of each of three independent plants per treatment ($n = 3$). The leaf discs were incubated in 10 mL of 99% methanol and kept in the dark at 25 ± 2 °C for 24 h to ensure complete pigment extraction.

The absorbance of the extracts was measured using a UV–Vis spectrophotometer (GENESYS™ 10S, Thermo Fisher Scientific, Madison, WI, USA) at 666, 653, and 470 nm, corresponding to chlorophyll a, chlorophyll b, and total carotenoids, respectively. Pigment concentrations were calculated using the following equations, expressing the results in micrograms per square centimeter of leaf area (µg cm^{-2}):

$$\text{Chl } a^* = [15.65\ (A666) - 7.34(A653)]$$

$$chlorophyll\ a = \frac{chl\ a^* \times Ve \times w_1}{w_2 \times \pi \times r^2 \times n} \quad (2)$$

$$\text{Chl } b^* = [27.05\ (A653) - 11.21(A666)]$$

$$chlorophyll\ b = \frac{chl\ b^* \times Ve \times w_1}{w_2 \times \pi \times r^2 \times n} \quad (3)$$

$$\text{Carotenoids}^* = ([(1000(A470)) - 2.86(chl\ a^*) - 129.2(chl\ b^*)])/((221))$$

$$carotenoids = \frac{carotenoids^* \times Ve \times w_1}{w_2 \times \pi \times r^2 \times n} \quad (4)$$

$$Total\ chorophyll = chl\ a^{*} + chl\ b^{*} \quad (5)$$

where $\boldsymbol{A}$: absorbance; $\boldsymbol{V_e}$: extraction volume; $\boldsymbol{W_1}$: weight per leaf disc; $\boldsymbol{W_2}$: total weight of leaf discs; $\boldsymbol{r}$: radius of leaf discs; $\boldsymbol{n}$: number of leaf discs.

2.8.5. Total Soluble Sugars and Proline Quantification

Total soluble sugars and proline were quantified from fresh leaf tissue collected from three independent plants per treatment ($n = 3$), following the methodology described by Irigoyen et al. [28]. Approximately 0.25–0.50 g of fresh leaf tissue was homogenized in 96% ethanol, followed by two successive washes with 70% ethanol to ensure complete extraction of soluble metabolites. The extracts were centrifuged at 5500 rpm for 10 min, and the resulting supernatant was used for the subsequent biochemical analyses.

Proline concentration was determined using the acid ninhydrin colorimetric assay, followed by benzene extraction and spectrophotometric measurement at 520 nm. Total soluble sugars were quantified from the same ethanolic extract using the anthrone–sulfuric acid colorimetric method. Absorbance was measured using a GENESYS™ 10S UV–Vis spectrophotometer (Thermo Fisher Scientific, Madison, WI, USA). The concentrations of proline and total soluble sugars were expressed as mg g^{-1} fresh weight (FW).

2.8.6. Mineral Analysis

Leaf samples from three independent plants per treatment ($n = 3$) were washed with distilled water, dried at 60 °C to constant weight, and ground to a fine powder. For mineral analysis, 1 g of dried leaf material was digested with 25 mL of a triacid mixture consisting of concentrated HNO_3, HCl, and H_2SO_4 (1000:100:25, $v/v/v$). After complete digestion, the samples were filtered and brought to a final volume of 50 mL with deionized water. The concentrations of Ca, K, Mg, Na, Cu, Fe, Mn, and Zn were quantified by inductively coupled plasma–optical emission spectrometry (ICP-OES; Agilent Technologies 700 Series, Santa Clara, CA, USA), following the analytical approach described by Ramírez-Estrada et al. [29]. Phosphorus (P) was determined colorimetrically using the ammonium vanadate–molybdate method [30]; briefly, a 5-mL aliquot of the digested extract was transferred to a 50-mL volumetric flask, mixed with 10 mL of ammonium vanadate–molybdate reagent, and brought to volume with deionized water. After 30 min of color development, absorbance was measured at 470 nm using a UV–Vis spectrophotometer (GENESYS™ 10S, Thermo Fisher Scientific, Madison, WI, USA). Mineral concentrations were expressed on a dry-weight basis.

Leaf mineral accumulation was calculated individually for each of the three plants per treatment by multiplying the mineral concentration by the corresponding leaf dry biomass obtained from the same plant. For P, K, Ca, and Mg, expressed as percentage of dry weight, *mineral accumulation* was calculated as *concentration* (%) × *leaf dry biomass* (g) × *10*. For Na, Fe, Zn, Mn, and Cu, expressed as mg kg^{-1} dry weight, *mineral accumulation* was calculated as *concentration* (mg kg^{-1}) × *leaf dry biomass* (g)/*1000*. All accumulation values were expressed as mg $plant^{-1}$. This approach allowed mineral concentration and leaf mineral accumulation to be evaluated separately, accounting for differences in leaf dry biomass among treatments.

2.9. Statistical Analysis

All variables were first assessed for normality and homogeneity of variances using the Shapiro–Wilk and Levene tests, respectively. Subsequently, data were subjected to one-way analysis of variance (ANOVA), with treatment as the main factor, using SAS 9.4 OnDemand for Academics (SAS Institute Inc., Cary, NC, USA). When a significant treatment effect was detected, means were separated using Fisher's least significant difference (LSD) test at $p \leq 0.05$. Different letters in tables and figures indicate significant differences among treat-

ments. The sample size used for statistical analysis corresponded to the number of biological replicates evaluated for each variable: six plants per treatment ($n = 6$) for biomass, fruit yield, gas exchange, chlorophyll fluorescence, and SPAD measurements, and three plants per treatment ($n = 3$) for biochemical and mineral analyses. Measurements obtained from the same plant were considered subsamples and were not treated as additional independent biological replicates.

Pearson correlation coefficients were calculated using individual plant observations. For the correlation matrix, 23 variables were evaluated using 24 complete observations (three plants per treatment), resulting in 253 nonredundant pairwise correlations. To control the false discovery rate associated with multiple comparisons, p-values were adjusted using the Benjamini–Hochberg procedure. Statistical significance was determined using the adjusted p-values (q-values), with thresholds of $q < 0.05$, $q < 0.01$, and $q < 0.001$. Correlation analyses were performed in Python 3.12 using SciPy and statsmodels.

Principal component analysis (PCA) was performed on 23 variables using complete observations ($n = 24$; three plants per treatment). Variables were standardized to z-scores prior to PCA. The first two principal components were used to visualize treatment scores and variable loadings. Pearson correlation analysis and PCA were performed in Python 3.12 using SciPy and scikit-learn, respectively.

3. Results

3.1. Physicochemical Characterization of Nanoparticles

According to the manufacturer's technical documentation, the ZnO nanoparticles had an average particle size of 50 nm and a nominal purity of 99.7%, while the SiO_2 nanoparticles had a particle size range of 70–90 nm. Transmission electron microscopy (TEM) micrographs, provided by the manufacturer, documented the morphology of the ZnO- and SiO_2-based materials (Figure 1A,B). The TEM images depict the materials as they appear in the supplier's documentation.

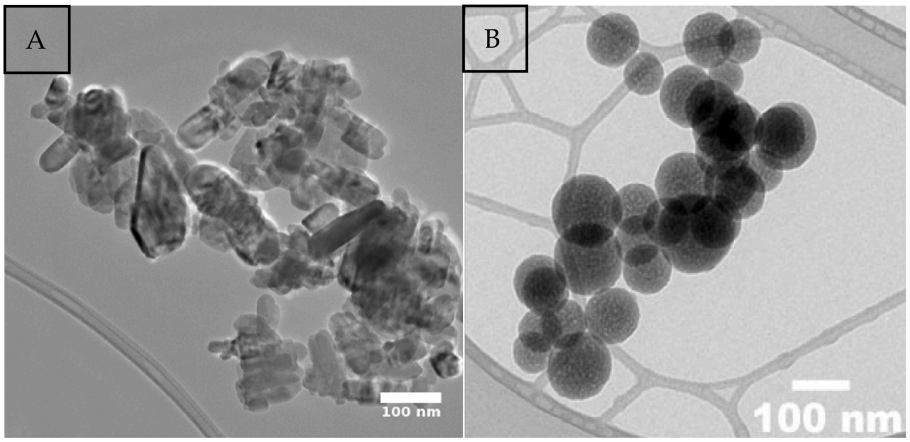


Figure 1. Manufacturer-supplied transmission electron microscopy (TEM) micrographs of (**A**) ZnO nanoparticles and (**B**) SiO_2 nanoparticles reproduced from the corresponding technical datasheets. These images document the supplier-reported materials and do not represent independent characterization of the final chitosan-containing foliar suspensions.

The documentation for the ZnO also indicated a hexagonal wurtzite structure determined via X-ray diffraction (XRD) and mentioned characterization by scanning electron microscopy (SEM) and energy-dispersive X-ray spectroscopy (EDX). In contrast, the documentation available for the SiO_2 nanoparticles did not include XRD or EDX results. These

properties correspond to specifications declared by the supplier and were not independently verified in the present study.

However, quantitative particle-size distributions, aggregation behavior, and suspension stability under the experimental preparation conditions were not independently determined.

3.2. Biomass Accumulation, Yield, and SPAD Index

Foliar treatments significantly affected leaf dry biomass, stem dry biomass, fruit dry biomass, aboveground dry biomass, fruit yield, and SPAD index ($p \leq 0.05$; Figure 2A–F). Leaf dry biomass remained relatively unchanged between Control-WW and Control-WL (−5.1%; Figure 2A), while ZnO NPs maintained the highest leaf biomass among the foliar treatments, with values statistically comparable to both controls. Stem dry biomass decreased significantly by 23.8% in Control-WL compared with Control-WW (Figure 2B); ZnO NPs produced the highest value among the foliar treatments, increasing stem biomass by 5.1% relative to Control-WL, although remaining 19.9% below Control-WW and statistically comparable to both controls.

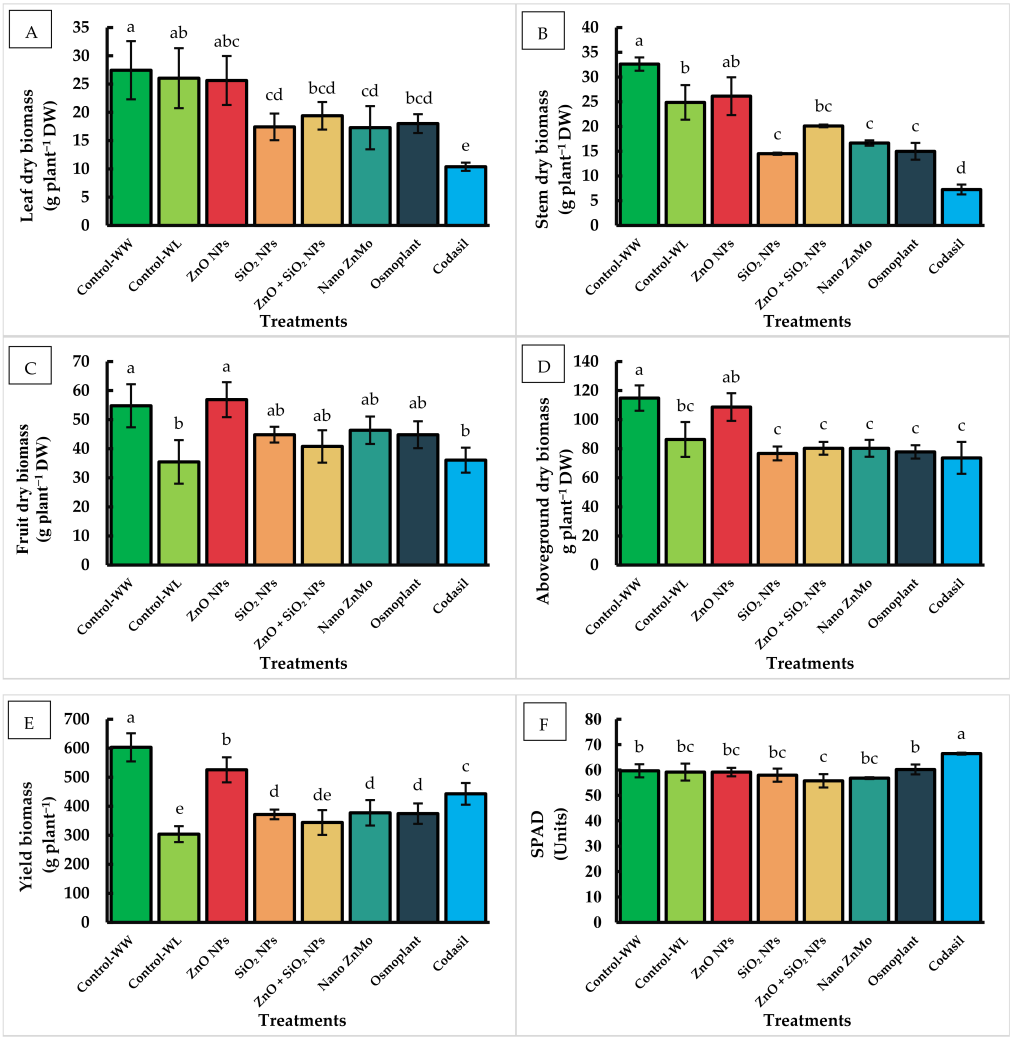


Figure 2. Effects of foliar treatments on growth, biomass accumulation, yield, and SPAD index of jalapeño pepper under severe water limitation. (**A**) Leaf dry biomass, (**B**) stem dry biomass, (**C**) fruit dry biomass, (**D**) aboveground dry biomass, (**E**) fruit yield, and (**F**) SPAD index. Bars represent the mean ± standard deviation ($n = 6$). Different letters above the bars indicate statistically significant differences among treatments, as determined by Fisher's LSD test ($p \leq 0.05$).

Fruit dry biomass decreased significantly by 35.2% in Control-WL compared with Control-WW (Figure 2C). ZnO NPs produced the highest fruit dry biomass among the foliar treatments, increasing it by 60.3% relative to Control-WL and reaching a level comparable to Control-WW. Aboveground dry biomass decreased significantly by 24.8% in Control-WL compared with Control-WW (Figure 2D), whereas ZnO NPs increased it by 25.7% relative to Control-WL, reaching a level only 5.4% below Control-WW.

Fruit yield exhibited the strongest response to water deficit, with Control-WL showing a 49.6% reduction relative to Control-WW (Figure 2E). ZnO NPs significantly increased yield by 72.8% relative to Control-WL, although it remained 12.8% below Control-WW.

Finally, SPAD remained unchanged between the two controls (−0.9%; Figure 2F), whereas Codasil produced the highest value, significantly exceeding Control-WW and Control-WL by 11.3 and 12.3%, respectively.

3.3. Leaf Gas Exchange

Gas exchange parameters were significantly affected by foliar treatments ($p < 0.001$; Figure 3A–D), whereas Control-WW and Control-WL did not differ significantly in any of the evaluated variables. All foliar treatments significantly increased net photosynthetic rate (P_N) relative to Control-WL (Figure 3A), with Codasil producing the strongest response (+57.1%) and exceeding Control-WW by approximately 57.5%. Stomatal conductance (gs) was reduced by several foliar treatments (Figure 3B), with Osmoplant showing the lowest value, 44.9% below Control-WL and approximately 51% below Control-WW. Similarly, SiO_2 NPs produced the largest decrease in intercellular CO_2 concentration (Ci), reducing it by 55.8% relative to Control-WL and approximately 57.5% relative to Control-WW (Figure 3C). Transpiration rate (E) followed a similar pattern (Figure 3D), with Osmoplant producing the greatest reduction, approximately 34% below Control-WL and 37% below Control-WW.

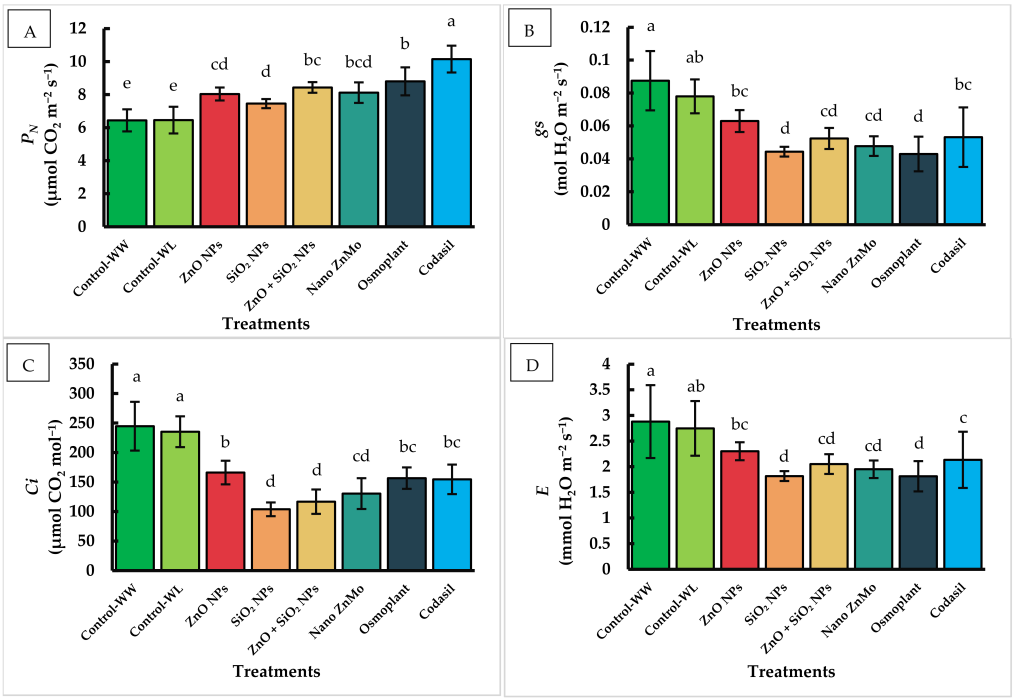


Figure 3. Effects of foliar treatments on gas exchange parameters of jalapeño pepper. (**A**) Net photosynthetic rate (P_N), (**B**) stomatal conductance (gs), (**C**) intercellular CO_2 concentration (Ci), (**D**) transpiration rate (E) under severe water limitation. Bars represent the mean ± standard deviation ($n = 6$). Different letters above the bars indicate statistically significant differences among treatments, as determined by Fisher's LSD test ($p \leq 0.05$).

3.4. Chlorophyll Fluorescence, Carboxylation Efficiency, and Water-Use Efficiency

Foliar treatments significantly affected Fv′/Fm′, photochemical quenching (qP), electron transport rate (ETR), leaf vapor pressure deficit (VpdL), carboxylation efficiency (CE), water-use efficiency (WUE), and intrinsic water-use efficiency (WUEi) ($p < 0.001$; Table 5). Compared with Control-WW, Control-WL significantly increased Fv′/Fm′ by 5.7%, whereas qP and ETR decreased by 35.3 and 32.3%, respectively. ZnO NPs produced the strongest response in Fv′/Fm′, increasing it by 5.4% relative to Control-WL and 11.4% relative to Control-WW. In contrast, Codasil produced the highest qP and ETR, increasing them by 112.6 and 90.2%, respectively, relative to Control-WL and by 37.5 and 28.7% relative to Control-WW. VpdL remained statistically unchanged between the two controls, whereas Osmoplant produced the highest value, increasing it by 18.0% relative to Control-WL and 23.8% relative to Control-WW.

Table 5. Effects of foliar treatments on chlorophyll fluorescence, carboxylation efficiency, and water-use efficiency of jalapeño pepper under severe water limitation.

Treatments	Fv′/Fm′	qP	ETR	VpdL	CE	WUE	WUEi
Control-WW	0.493 ± 0.004 ^{cd}	0.283 ± 0.067 ^{d}	81.95 ± 19.29 ^{bc}	3.02 ± 0.31 ^{d}	0.027 ± 0.003 ^{d}	2.34 ± 0.49 ^{c}	80.86 ± 26 ^{e}
Control-WL	0.521 ± 0.018 ^{b}	0.183 ± 0.054 ^{bc}	55.46 ± 14.40 ^{d}	3.17 ± 0.25 ^{d}	0.028 ± 0.003 ^{d}	2.39 ± 0.26 ^{c}	86.30 ± 16 ^{e}
ZnO NPs	0.549 ± 0.012 ^{a}	0.256 ± 0.056 ^{bc}	82.84 ± 19.36 ^{bc}	3.23 ± 0.09 ^{cd}	0.049 ± 0.007 ^{c}	3.51 ± 0.26 ^{b}	128.64 ± 12 ^{d}
SiO_2 NPs	0.475 ± 0.013 ^{de}	0.316 ± 0.051 ^{b}	87.96 ± 12.41 ^{ab}	3.58 ± 0.04 ^{ab}	0.073 ± 0.008 ^{a}	4.11 ± 0.14 ^{b}	168.53 ± 7 ^{bc}
ZnO + SiO_2 NPs	0.509 ± 0.017 ^{bc}	0.232 ± 0.043 ^{cd}	69.34 ± 12.13 ^{cd}	3.44 ± 0.14 ^{bc}	0.074 ± 0.012 ^{a}	4.13 ± 0.36 ^{b}	162.48 ± 15 ^{cd}
Nano ZnMo	0.498 ± 0.009 ^{c}	0.226 ± 0.077 ^{cd}	66.28 ± 23.13 ^{cd}	3.59 ± 0.12 ^{ab}	0.064 ± 0.008 ^{ab}	4.18 ± 0.37 ^{b}	171.65 ± 19 ^{bc}
Osmoplant	0.500 ± 0.016 ^{c}	0.221 ± 0.004 ^{cd}	64.82 ± 3.23 ^{cd}	3.74 ± 0.26 ^{a}	0.057 ± 0.008 ^{bc}	4.99 ± 1.10 ^{a}	216.73 ± 60 ^{a}
Codasil	0.464 ± 0.035 ^{e}	0.389 ± 0.054 ^{a}	105.50 ± 11.90 ^{a}	3.60 ± 0.30 ^{ab}	0.068 ± 0.018 ^{a}	4.96 ± 1.01 ^{a}	207.30 ± 59 ^{ab}

Values represent the mean ± standard deviation ($n = 6$). Different letters within each column indicate statistically significant differences among treatments, as determined by Fisher's LSD test ($p \leq 0.05$).

CE was also similar between Control-WW and Control-WL, while ZnO + SiO_2 NPs produced the strongest response, increasing CE by 164.3% relative to Control-WL and 174.1% relative to Control-WW. Similarly, WUE and WUEi remained unchanged between the two controls, whereas Osmoplant produced the highest values, increasing WUE and WUEi by 108.8 and 151.1%, respectively, relative to Control-WL and by 113.2 and 168.0% relative to Control-WW.

3.5. Photosynthetic Pigments, Total Soluble Sugars and Proline

Foliar treatments significantly affected carotenoid content, total soluble sugars, and proline concentration ($p \leq 0.05$; Figure 4A–D). Total chlorophyll remained statistically unchanged between Control-WW and Control-WL (+8.7%; Figure 4A), with SiO_2 NPs showing the highest numerical value among the foliar treatments and remaining comparable to both controls. Carotenoid content was also similar between the two controls (Figure 4B), whereas ZnO NPs produced the strongest response, increasing carotenoids by 78.3% relative to Control-WL and 101.9% relative to Control-WW.

Total soluble sugars decreased significantly by 40.5% in Control-WL compared with Control-WW (Figure 4C), whereas ZnO + SiO_2 NPs increased their concentration by 42.4% relative to Control-WL, although remaining 15.3% below Control-WW. Proline concentration decreased significantly by 34.6% in Control-WL relative to Control-WW (Figure 4D). SiO_2 NPs showed the highest numerical proline concentration among the foliar treatments, 24.0% above Control-WL, although this increase was not statistically significant and remained statistically comparable to both controls.

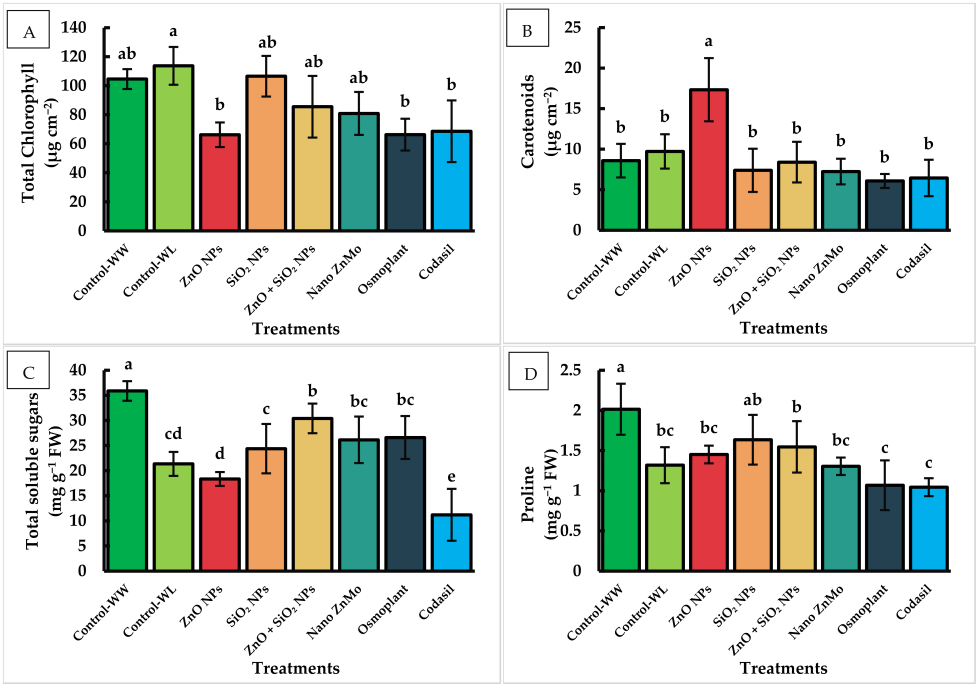


Figure 4. Effects of foliar treatments on (**A**) Total Chlorophyll, (**B**) Carotenoids, (**C**) Total soluble sugars, (**D**) proline under severe water limitation. Bars represent the mean ± standard deviation ($n = 3$). Different letters above the bars indicate statistically significant differences among treatments, as determined by Fisher's LSD test ($p \leq 0.05$).

3.6. Leaf Mineral Concentration and Accumulation

Leaf mineral concentration and accumulation provide complementary information on nutrient status and biomass-associated mineral retention under water-limited conditions. Foliar treatments significantly affected the concentrations of P, K, Ca, Mg, Na, Fe, Zn, Mn, and Cu ($p \leq 0.05$; Table 6). P and K concentrations remained statistically comparable between Control-WW and Control-WL, with Nano ZnMo showing the highest P concentration and SiO_2 NPs and Osmoplant maintaining the highest K concentrations among the foliar treatments. In contrast, Control-WL significantly increased Ca, Mg, Zn, and Mn concentrations relative to Control-WW, whereas Na and Fe concentrations decreased. Among the foliar treatments, Osmoplant maintained the highest Ca and Mn concentrations, ZnO NPs showed the highest Mg concentration, and ZnO + SiO_2 NPs produced the lowest Na concentration. Nano ZnMo increased Fe concentration by 55.7% relative to Control-WL, reaching a level statistically comparable to Control-WW, while Nano ZnMo and SiO_2 NPs showed the highest Zn concentrations among the foliar treatments. Cu concentration remained statistically comparable between the two controls, although Nano ZnMo showed the highest mean concentration among the foliar treatments (Table 6).

Because mineral concentration does not necessarily reflect the total quantity of an element retained in plant tissues, leaf mineral accumulation was calculated using the corresponding mineral concentration and leaf dry biomass of each plant (Table 7). Significant treatment effects were detected for P, K, Mg, Na, Fe, Zn, and Mn accumulation ($p \leq 0.05$), whereas Ca and Cu accumulation did not differ significantly among treatments. Control-WW showed the highest P and K accumulation, while Codasil exhibited the lowest values for both elements. ZnO NPs produced the highest mean Mg accumulation (239 mg plant^{-1}), statistically comparable to Control-WL and Control-WW. Na accumulation was significantly lower in Control-WL than in Control-WW, with the lowest statistical group observed in SiO_2 NPs, ZnO + SiO_2 NPs, Osmoplant, and Codasil.

Table 6. Effects of foliar treatments on the mineral composition of jalapeño pepper under severe water limitation.

Treatments	P (%)	K (%)	Ca (%)	Mg (%)	Na ppm	Fe ppm	Zn ppm	Mn ppm	Cu ppm
Control-WW	0.32 ± 0.03 ^{a}	3.9 ± 0.1 ^{a}	1.2 ± 0.3 ^{b}	0.73 ± 0.06 ^{c}	10.4 ± 0.2 ^{a}	87.3 ± 6.9 ^{a}	13.0 ± 1.0 ^{d}	76.4 ± 3.8 ^{f}	6.1 ± 0.7 ^{bc}
Control-WL	0.29 ± 0.03 ^{ab}	3.5 ± 0.1 ^{ab}	2.2 ± 0.1 ^{a}	0.88 ± 0.04 ^{ab}	8.1 ± 1.1 ^{b}	52.4 ± 1.2 ^{cd}	90.3 ± 12.6 ^{c}	151.5 ± 9.7 ^{de}	8.8 ± 3.1 ^{ab}
ZnO NPs	0.28 ± 0.03 ^{ab}	3.0 ± 1.1 ^{b}	1.6 ± 0.7 ^{ab}	0.93 ± 0.02 ^{a}	6.8 ± 1.5 ^{bcd}	50.0 ± 1.1 ^{d}	81.2 ± 1.0 ^{c}	150.1 ± 0.1 ^{e}	6.7 ± 2.1 ^{bc}
SiO_2 NPs	0.24 ± 0.03 ^{bc}	3.8 ± 0.2 ^{a}	1.7 ± 0.7 ^{ab}	0.91 ± 0.05 ^{a}	5.6 ± 1.2 ^{cd}	63.7 ± 3.7 ^{b}	132.5 ± 9.5 ^{a}	175.6 ± 27.1 ^{c}	7.4 ± 1.9 ^{abc}
ZnO + SiO_2 NPs	0.27 ± 0.07 ^{ab}	3.5 ± 0.1 ^{ab}	1.4 ± 0.6 ^{ab}	0.88 ± 0.04 ^{ab}	4.8 ± 1.1 ^{d}	61.4 ± 5.0 ^{bc}	113.2 ± 5.2 ^{b}	197.0 ± 8.4 ^{ab}	5.1 ± 1.1 ^{c}
Nano ZnMo	0.32 ± 0.05 ^{a}	3.7 ± 0.4 ^{a}	1.5 ± 0.5 ^{ab}	0.76 ± 0.16 ^{bc}	6.8 ± 1.2 ^{bc}	81.6 ± 11.2 ^{a}	136.8 ± 2.6 ^{a}	184.3 ± 10.8 ^{b}	10.2 ± 3.0 ^{a}
Osmoplant	0.18 ± 0.01 ^{cd}	3.8 ± 0.2 ^{a}	2.2 ± 0.1 ^{a}	0.82 ± 0.11 ^{abc}	4.9 ± 0.6 ^{cd}	51.4 ± 2.9 ^{d}	113.4 ± 15.7 ^{b}	215.9 ± 1.2 ^{a}	6.0 ± 2.0 ^{bc}
Codasil	0.16 ± 0.04 ^{d}	3.6 ± 0.1 ^{ab}	1.6 ± 0.2 ^{ab}	0.71 ± 0.01 ^{c}	5.9 ± 1.6 ^{cd}	52.2 ± 4.1 ^{cd}	75.8 ± 10.4 ^{c}	170.9 ± 3.9 ^{cd}	6.5 ± 0.8 ^{bc}

Values represent the mean ± standard deviation ($n = 3$). Different letters within each column indicate statistically significant differences among treatments, as determined by Fisher'sLSD test ($p \leq 0.05$).

Table 7. Effects of foliar treatments on leaf mineral accumulation in jalapeño pepper under severe water limitation.

Treatments	P	K	Ca	Mg	Na (mg plant^{-1})	Fe	Zn	Mn	Cu
Control-WW	84 ± 17 ^{a}	1059 ± 196 ^{a}	315 ± 26 ^{a}	197 ± 21 ^{abc}	0.286 ± 0.048 $_{a}$	2.420 ± 0.638 $_{a}$	0.353 ± 0.040 $_{b}$	2.085 ± 0.290 $_{bc}$	0.166 ± 0.014 $_{a}$
Control-WL	72 ± 23 ^{ab}	917 ± 355 ^{ab}	573 ± 251 ^{a}	228 ± 85 ^{ab}	0.204 ± 0.058 $_{b}$	1.374 ± 0.589 $_{b}$	2.443 ± 1.292 $_{a}$	3.878 ± 1.362 $_{a}$	0.251 ± 0.177 $_{a}$
ZnO NPs	69 ± 4.5 ^{ab}	768 ± 306 ^{ab}	379 ± 105 ^{a}	239 ± 41 ^{a}	0.179 ± 0.069 $_{bc}$	1.286 ± 0.246 $_{b}$	2.084 ± 0.377 $_{a}$	3.847 ± 0.649 $_{a}$	0.166 ± 0.025 $_{a}$
SiO_2 NPs	39 ± 8.2 ^{cd}	659 ± 122 ^{bc}	314 ± 155 ^{a}	158 ± 13 ^{cd}	0.099 ± 0.034 $_{d}$	1.105 ± 0.085 $_{bc}$	2.295 ± 0.147 $_{a}$	3.019 ± 0.069 $_{ab}$	0.126 ± 0.016 $_{a}$
ZnO + SiO_2 NPs	57 ± 21 ^{bc}	682 ± 95 ^{bc}	289 ± 151 ^{a}	171 ± 14 ^{bcd}	0.095 ± 0.033 $_{d}$	1.200 ± 0.247 $_{b}$	2.205 ± 0.376 $_{a}$	3.809 ± 0.317 $_{a}$	0.101 ± 0.033 $_{a}$
Nano ZnMo	52 ± 15 ^{bc}	637 ± 74 ^{bc}	259 ± 123 ^{a}	128 ± 4 ^{de}	0.115 ± 0.006 $_{cd}$	1.383 ± 0.121 $_{b}$	2.360 ± 0.479 $_{a}$	3.160 ± 0.519 $_{a}$	0.169 ± 0.014 $_{a}$
Osmoplant	33 ± 4.5 ^{d}	678 ± 94 ^{bc}	397 ± 32 ^{a}	147 ± 6 ^{cd}	0.089 ± 0.019 $_{d}$	0.923 ± 0.033 $_{bc}$	2.061 ± 0.472 $_{a}$	3.891 ± 0.381 $_{a}$	0.110 ± 0.046 $_{a}$
Codasil	17 ± 5.5 ^{d}	375 ± 13 ^{c}	164 ± 10 ^{a}	74 ± 6 ^{e}	0.060 ± 0.012 $_{d}$	0.540 ± 0.005 $_{c}$	0.792 ± 0.162 $_{b}$	1.776 ± 0.164 $_{c}$	0.067 ± 0.004 $_{a}$

Values represent the mean ± standard deviation ($n = 3$). Different letters within each column indicate statistically significant differences among treatments, as determined by Fisher's LSD test ($p \leq 0.05$).

Fe accumulation decreased significantly in Control-WL relative to Control-WW, from 2.42 to 1.37 mg plant^{-1} (Table 7). Although Nano ZnMo increased Fe concentration relative to Control-WL (Table 6), its Fe accumulation (1.38 mg plant^{-1}) remained statistically comparable to Control-WL, indicating that the concentration increase was not accompanied by greater foliar Fe accumulation. Conversely, Zn accumulation increased markedly in Control-WL relative to Control-WW, from 0.35 to 2.44 mg plant^{-1}, with all foliar treatments except Codasil maintaining values statistically comparable to Control-WL. Mn accumulation also increased under water-limited conditions, with Osmoplant, Control-WL, ZnO NPs, and ZnO + SiO_2 NPs showing the highest mean values, whereas Codasil exhibited the lowest accumulation. These results demonstrate that changes in leaf mineral concentration were not consistently accompanied by corresponding changes in mineral accumulation, emphasizing the importance of considering leaf biomass when evaluating treatment-associated nutritional responses.

3.7. Heat Map and Correlation Analysis

Pearson correlation analysis revealed distinct associations among growth, yield, photosynthetic, biochemical, and mineral traits after Benjamini–Hochberg false discovery rate (FDR) correction (Figure 5). Aboveground dry biomass was positively correlated with fruit yield ($r = 0.73$, $q < 0.001$), stomatal conductance (gs; $r = 0.58$, $q < 0.05$), and transpiration rate (E; $r = 0.55$, $q < 0.05$), whereas a negative correlation was observed with Mn ($r = -0.67$, $q < 0.01$). Among photosynthetic traits, gs was strongly correlated with E ($r = 0.99$, $q < 0.001$), while photochemical quenching (qP) was closely associated with elec-

tron transport rate (ETR; $r = 0.96$, $q < 0.001$). Net photosynthetic rate (P_N) was negatively correlated with total soluble sugars ($r = -0.61$, $q < 0.05$), whereas its associations with ETR, qP, and SPAD did not remain significant after FDR correction. Fruit yield was positively correlated with ETR ($r = 0.61$, $q < 0.05$), whereas negative correlations were observed with Zn ($r = -0.67$, $q < 0.01$) and Mn ($r = -0.67$, $q < 0.01$). Among mineral nutrients, Mn and Zn were strongly positively correlated ($r = 0.84$, $q < 0.001$), whereas Mn-Na ($r = -0.82$, $q < 0.001$) and Zn-Na ($r = -0.69$, $q < 0.01$) showed strong negative associations. These results indicate that biomass and yield were associated with selected gas exchange and photochemical traits, while Zn and Mn exhibited inverse relationships with productivity under the evaluated conditions.

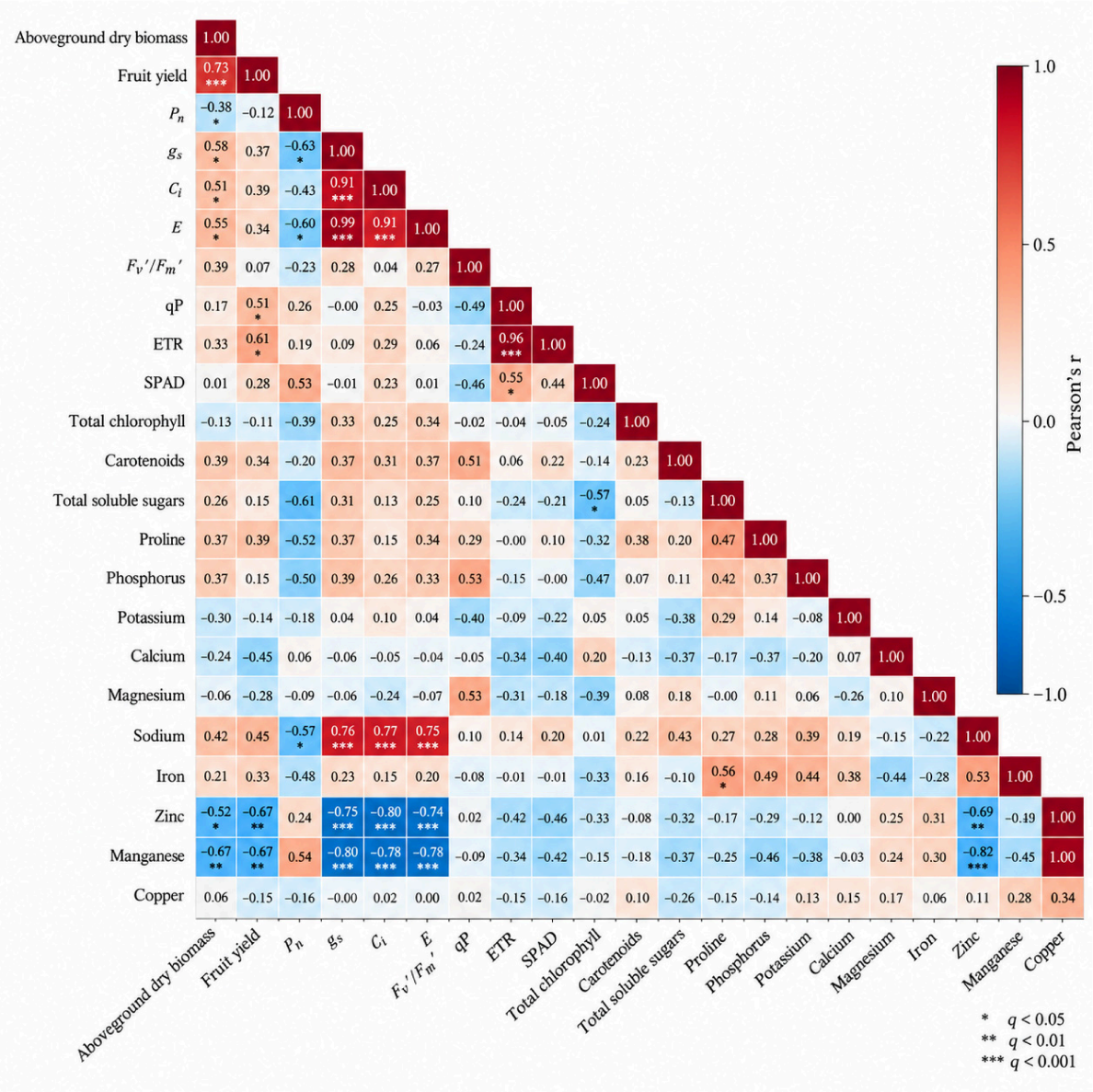


Figure 5. Pearson correlation matrix among growth, yield, photosynthetic, biochemical, and mineral traits of jalapeño pepper under water-limited conditions. Cell colors indicate the direction and magnitude of Pearson's correlation coefficients (r), ranging from −1 to +1. Correlations were calculated using 24 individual plant observations ($n = 24$). Statistical significance was determined after Benjamini-Hochberg false discovery rate (FDR) correction for multiple comparisons (* $q < 0.05$, ** $q < 0.01$, and *** $q < 0.001$).

3.8. Principal Component Analysis (PCA)

Principal component analysis clearly differentiated the multivariate response patterns among treatments (Figure 6A,B). PC1 explained 32.31% of the total variance and PC2 explained 17.61%, together accounting for 49.92% of the variability in the dataset. The score distribution showed that Control-WW was the most clearly separated group along positive PC1, whereas Codasil was distinctly separated along positive PC2 (Figure 6A). ZnO NPs were also positioned toward positive PC1, while SiO_2 NPs, ZnO + SiO_2 NPs, Nano ZnMo, and Osmoplant were predominantly distributed toward negative PC1, with partial overlap among their treatment ellipses. Control-WL occupied an intermediate position characterized by positive PC1 and negative PC2 scores. The loading analysis showed that positive PC1 was primarily associated with stomatal conductance (*gs*), transpiration rate (*E*), Na, intercellular CO_2 concentration (*Ci*), aboveground dry biomass, and fruit yield, whereas Mn, Zn, and net photosynthetic rate (P_N) were oriented toward negative PC1 (Figure 6B). Positive PC2 was mainly associated with SPAD, photochemical quenching (qP), electron transport rate (ETR), and P_N, while Fv'/Fm' total soluble sugars, and P were oriented toward negative PC2. Accordingly, the separation of Control-WW along positive PC1 coincided primarily with gas exchange, biomass, and yield traits, whereas the separation of Codasil along positive PC2 was more closely associated with photosynthetic and photochemical traits.

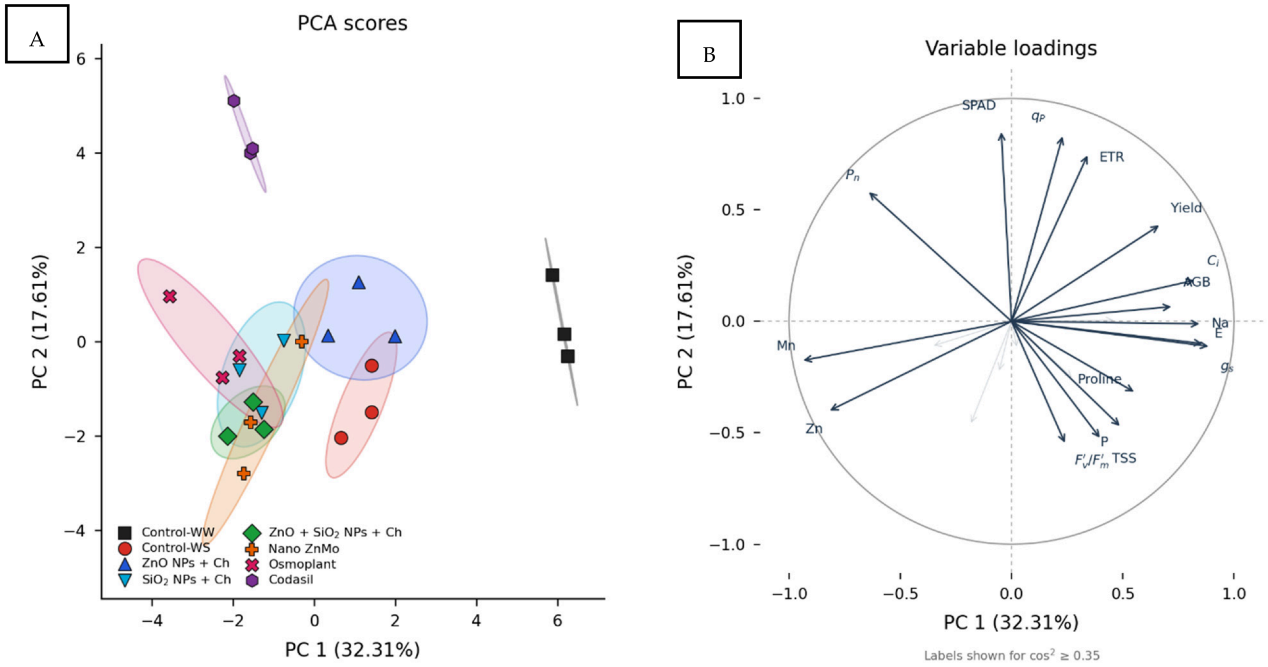


Figure 6. Principal component analysis (PCA) of growth, yield, physiological, biochemical, and mineral traits of jalapeño pepper across foliar treatments and irrigation conditions. (**A**) PCA score plot showing the distribution of individual observations and descriptive covariance ellipses for each treatment. (**B**) Variable loading plot showing the direction and magnitude of the associations of the evaluated traits with PC1 and PC2. PC1 and PC2 explained 32.31 and 17.61% of the total variance, respectively, accounting for 49.92% of the cumulative variance. All 23 standardized variables were included in the analysis; for clarity, labels are displayed for variables with $\cos^2 \geq 0.35$, while lighter arrows represent the remaining variables.

4. Discussion

Biomass accumulation and its distribution among plant organs integrate resource acquisition and dry-matter allocation, making them important indicators of plant perfor-

mance under limited water availability [31]. In this study, Control-WW maintained the highest overall productive performance, whereas severe water limitation in Control-WL particularly restricted stem, fruit, and aboveground dry biomass, resulting in the greatest decline in fruit yield, while leaf biomass remained comparatively stable (Figure 2A–E). This pattern indicates that reproductive productivity was more sensitive to restricted water availability than leaf biomass maintenance. Consistently, reduced irrigation has been shown to compromise fruit yield in *Capsicum annuum* L., although the magnitude of this response depends on genotype [32]. Among the foliar treatments, ZnO NPs showed the strongest capacity to counteract these limitations, maintaining fruit dry biomass at a level comparable to Control-WW while substantially recovering aboveground biomass and fruit yield relative to Control-WL (Figure 2C–E). This response is consistent with improvements in biomass and plant water status reported for ZnO NP-treated *Capsicum annuum* under restricted water availability [33], as well as with enhanced productivity following foliar ZnO NP application in field-grown soybean [34]. These findings suggest that ZnO NPs helped sustain reproductive growth and productive biomass formation under severe water limitation. However, the physiological mechanisms underlying this improvement could not be fully established from the measured variables, and the observed associations should not be interpreted as direct evidence of causality. Although cumulative fruit yield and organ-specific biomass were directly quantified, individual yield components, including fruit number, mean fruit weight, and fruit set, were not assessed. Therefore, the observed yield recovery cannot be attributed to specific changes in fruit number or size, and further studies are needed to elucidate the underlying yield components.

In contrast, SPAD remained similar between Control-WW and Control-WL, whereas Codasil produced the highest SPAD value without a corresponding superiority in biomass or fruit yield (Figure 2F), indicating that maintenance of leaf chlorophyll status alone was insufficient to ensure greater reproductive productivity. Silicon supplementation has been associated with maintaining chlorophyll content in pepper under restricted water availability by suppressing chlorophyll degradation processes [35]. However, because Codasil is a multicomponent formulation containing silicon, amino acids, and potassium, its effect on SPAD cannot be attributed exclusively to silicon. Thus, the greater leaf greenness observed with Codasil did not translate into superior reproductive productivity under severe water limitation. These productive responses were accompanied by distinct changes in leaf physiological performance. Leaf gas exchange reflects the coordination between photosynthetic carbon assimilation and stomatal control of CO_2 uptake and transpirational water loss, a relationship that can be markedly modified under severe water limitation [36]. In this study, Control-WW and Control-WL maintained comparable net photosynthetic rate (P_N), stomatal conductance (g_s), intercellular CO_2 concentration (C_i), and transpiration rate (E), indicating that instantaneous gas exchange capacity was maintained at the evaluated stage despite the cumulative reductions in biomass and yield observed under severe water limitation (Figure 3A–D). This response should therefore be interpreted as the physiological status at the time of measurement rather than as evidence that carbon and water exchange remained unchanged throughout the crop cycle. Indeed, gas exchange responses to restricted water availability can differ according to the intensity and physiological context of the limitation. Asargew et al. [36] showed that severe water limitation altered the relationship between photosynthesis and stomatal conductance, whereas Padilla et al. [37] reported increased instantaneous and intrinsic water-use efficiency in pepper through enhanced stomatal regulation during short-term water limitation. In contrast to the irrigation controls, all foliar treatments increased P_N relative to Control-WL, while several treatments simultaneously reduced g_s, C_i, and E; Codasil produced the highest P_N, Osmoplant the strongest reductions in g_s and E, and SiO_2 NPs the lowest C_i (Figure 3A–D).

A comparable enhancement in CO_2 assimilation was observed in field-grown tomato under deficit irrigation, with ZnO NPs among the Fe and Zn based foliar treatments that increased the photosynthetic rate [38]. Similarly, Francesca et al. [39] found that a protein hydrolysate increased P_N under limited water availability in the E42 tomato genotype, although the response was genotype dependent. Thus, the contrasting responses between P_N and stomatal variables indicate treatment-dependent differences in carbon assimilation and transpirational water loss, although the underlying regulatory mechanisms could not be directly established from the measurements performed. Beyond stomatal regulation, the foliar treatments also modified PSII photochemical performance.

Chlorophyll fluorescence provides a sensitive assessment of PSII photochemistry, as water limitation can markedly alter the proportion of open PSII reaction centers and electron transport, reflected in changes in qP and ETR [40]. In this study, Control-WL exhibited higher Fv'/Fm' than Control-WW, whereas qP and ETR were markedly lower, indicating that the greater efficiency of excitation energy capture by open PSII reaction centers in the light-adapted state was not accompanied by greater photochemical utilization or electron transport under severe water limitation (Table 5). This contrasting response reinforces the importance of interpreting fluorescence parameters collectively rather than relying on a single index. Indeed, Zahedi et al. [41] observed that SiO_2 and SiO_2-NPs partially preserved Fv and Fm in strawberry under restricted water availability, whereas Fv'/Fm' showed comparatively low sensitivity, highlighting the differential responses of individual fluorescence parameters. Among the foliar treatments, ZnO NPs produced the highest Fv'/Fm', whereas Codasil maximized qP and ETR (Table 5), suggesting differential effects on excitation-use efficiency and the fraction of PSII reaction centers participating in photochemistry. Consistently, nano-Si and nano-Zn increased Fv/Fm and Φ_{PSII} in coriander grown under restricted water availability [42]. These findings reflect the instantaneous photosynthetic and photochemical responses measured at 45 DAT, providing insight into treatment-associated physiological differences under water-limited conditions.

Carboxylation efficiency and water-use efficiency provide complementary information on carbon fixation relative to internal CO_2 availability and water loss, respectively. In this study, CE remained comparable between Control-WW and Control-WL but was maximized by ZnO + SiO_2 NPs, whereas WUE and WUEi were also unchanged between the controls and reached their highest values with Osmoplant (Table 5). The divergent responses of CE and WUE indicate that enhanced carbon fixation relative to C_i did not necessarily coincide with the greatest efficiency of carbon gain relative to water loss. A similar dissociation was reported by Liu et al. [43], who found that SiO_2 NPs increased the instantaneous Rubisco carboxylation rate but decreased WUE under water-limited conditions. In the present study, the superior WUE and WUEi of Osmoplant are consistent with its combination of enhanced P_N relative to Control-WL and strong reductions in E and g_s, indicating tighter coordination between carbon assimilation and transpirational water loss under severe water limitation. These photosynthetic responses were accompanied by differential changes in pigment stability and osmotic adjustment.

Chlorophyll status reflects the integrity of the photosynthetic apparatus, whereas compatible solutes such as proline contribute to osmoprotection and cellular adjustment under restricted water availability [44]. In this study, total chlorophyll and carotenoid concentrations remained comparable between Control-WW and Control-WL, indicating that the leaf pigment pool was largely maintained at the evaluated stage despite severe water limitation (Figure 4A,B). This response contrasts with the progressive decline in total chlorophyll reported in *Capsicum frutescens* under prolonged irrigation withdrawal, in which pigment loss became increasingly pronounced with the duration of water limitation [44]. Among the foliar treatments, ZnO NPs produced the strongest carotenoid response, whereas

SiO_2 NPs showed only a numerical increase in total chlorophyll (Figure 4A,B). Consistently, foliar application of ZnO NPs increased carotenoid content in sugar beet under restricted water availability [45], supporting the capacity of ZnO NPs to enhance the carotenoid pool under water-limited conditions.

In contrast, Control-WL showed lower total soluble sugars and proline than Control-WW, while ZnO + SiO_2 NPs partially restored soluble sugars and SiO_2 NPs produced the highest numerical proline concentration without a significant increase over Control-WL (Figure 4C,D). This response differs from that reported in water-limited *Capsicum annuum* L., where soluble sugars and proline accumulated in response to restricted water availability [46]. However, proline accumulation should not be interpreted independently as a direct indicator of improved physiological performance. In chiltepin pepper, severe water limitation strongly increased proline in untreated plants, whereas effective *Bacillus* treatments reduced proline relative to the water-limited control while simultaneously improving leaf relative water content [47]. Thus, the lower proline observed in the present study does not necessarily indicate a weaker adaptive response; rather, it suggests that osmolyte accumulation was not the predominant physiological adjustment at the stage of severe water limitation evaluated. In addition to these physiological adjustments, severe water limitation and foliar treatments altered mineral nutrient composition.

Mineral nutrition is closely linked to plant physiological performance, and restricted water availability can alter nutrient transport, root acquisition, and tissue mineral composition [48]. In this study, Control-WW and Control-WL showed element-specific responses, with relatively stable P, K, and Cu concentrations, increased Ca, Mg, Zn, and Mn concentrations, and decreased Na and Fe concentrations under water-limited conditions (Table 6). However, these concentration patterns were not consistently reflected in leaf mineral accumulation (Table 7). Although Ca concentration increased under water limitation, Ca accumulation remained statistically unchanged, suggesting that concentration differences did not necessarily correspond to greater mineral retention in leaf tissues. Conversely, Zn and Mn showed higher concentrations accompanied by greater leaf accumulation, whereas Fe accumulation decreased significantly in Control-WL. These contrasting responses emphasize the importance of evaluating both mineral concentration and accumulation when interpreting plant nutritional status. Similar element-specific responses have been reported in *Capsicum annuum* L. Maphalaphathwa and Nciizah [49] observed that soil moisture did not significantly affect N, P, or K uptake, whereas Zn uptake depended on the interaction between moisture availability and nutrient priming. Conversely, Bitik et al. [48] reported declining mineral concentrations in pepper shoots under restricted water availability, while Martins et al. [50] observed reductions in several mineral elements in pepper fruits under 50% ETc.

Among the foliar treatments, Nano ZnMo maintained P and Fe concentrations comparable to Control-WW and showed high Zn concentrations (Table 6). However, its Fe accumulation remained statistically comparable to Control-WL, indicating that the increased Fe concentration was not accompanied by greater leaf Fe accumulation (Table 7). Similarly, Osmoplant produced the highest Ca and Mn concentrations among the foliar treatments, although Ca accumulation did not differ significantly among treatments. In contrast, ZnO NPs showed the highest mean Mg accumulation, whereas Nano ZnMo, SiO_2 NPs, and several other foliar formulations maintained Zn accumulation comparable to Control-WL (Table 7). Because Zn is a component of the Nano ZnMo formulation, its elevated foliar concentration should be interpreted partly in relation to direct Zn supply rather than exclusively as enhanced endogenous nutrient acquisition. Comparable treatment-dependent mineral responses have been reported by Al-Selwey et al. [51], who observed changes in the mineral composition of potato leaves following foliar ZnO and SiO_2 nanoparticle applications

under restricted water availability. Likewise, Martins et al. [50] reported treatment-specific changes in the mineral composition of pepper fruits under 50% ETc. Therefore, the present results indicate that foliar formulations modified mineral concentration and accumulation differently across elements, without demonstrating a generalized improvement in nutrient acquisition under water-limited conditions.

To integrate these individual responses, correlation and multivariate analyses were used to identify coordinated relationships among morphological, physiological, and biochemical traits associated with plant performance under limited water availability [52]. In this study, aboveground dry biomass was positively associated with fruit yield, stomatal conductance (gs), and transpiration rate (E), whereas fruit yield showed positive associations with selected physiological traits after FDR correction (Figure 5). The strong positive correlation between photochemical quenching (qP) and electron transport rate (ETR) indicates coordinated variation in PSII photochemical activity, although their relationships with net photosynthetic rate (P_N) were not statistically significant after correction for multiple comparisons. These findings suggest that photochemical performance, carbon assimilation, and productivity exhibited distinct patterns of association across treatments rather than a uniform physiological response. The importance of considering multiple physiological responses simultaneously is also evident in *Capsicum annuum* L., where reduced irrigation decreased yield and markedly altered stomatal conductance and leaf water potential [53]. Similarly, Raza et al. [54] showed through PCA that Cu-NP-mediated improvements in wheat productivity under restricted water availability were accompanied by changes in growth, WUE, chlorophyll status, stomatal conductance, and plant water relations.

The PCA further showed that the foliar treatments did not converge toward a single physiological response pattern (Figure 6A,B). Control-WW was positioned primarily in association with g_s, E, C_i, aboveground dry biomass, and fruit yield, whereas ZnO NPs were also oriented toward positive PC1, consistent with their comparatively strong productive performance under severe water limitation. In contrast, Codasil separated along positive PC2 in association with SPAD, qP, ETR, and P_N, indicating a predominantly photosynthetic and photochemical response that did not translate proportionally into the highest fruit yield (Figure 6A,B). This distinction indicates that enhancing instantaneous photosynthetic traits does not necessarily produce an equivalent improvement in cumulative productivity. Consistently, Liang et al. [55] showed that SiNP-mediated yield improvement in field-grown maize resulted from coordinated enhancement of leaf photosynthesis and canopy light interception rather than from the response of a single physiological trait. Finally, the negative correlations between Zn and Mn and biomass and yield, together with their opposite orientation relative to productive traits in the PCA, should be interpreted as treatment-dependent covariation rather than as evidence that these nutrients directly constrained productivity (Figures 5 and 6). These multivariate patterns indicate that productive performance under severe water limitation resulted from the coordination of biomass accumulation, gas exchange, and photochemical functioning rather than from the maximization of any single physiological or mineral trait.

The contrasting responses among nanoparticle-based formulations and commercial biostimulants should also be considered in relation to their different chemical compositions. Nano ZnMo supplied Zn and Mo together with seaweed-derived chelating agents, whereas Osmoplant provided amino acids, nitrogen, and potassium, and Codasil supplied silicon, amino acids, and potassium. Therefore, differences in physiological and productive performance among these treatments may reflect their overall formulation composition rather than nanoparticle-specific properties alone.

An important limitation of this study is that the observed responses reflect the effects of the complete foliar formulations rather than the isolated action of their individual

components. The ZnO- and SiO_2-based treatments contained chitosan as a stabilizing and dispersing agent, whereas the commercial formulations supplied additional nutrients and bioactive compounds. Because carrier-only, chitosan-only, and nutrient-equivalent controls were not included, the specific contributions of nanoparticle properties, chitosan, and other formulation components could not be independently determined. Therefore, the observed physiological and productive responses should be interpreted as treatment-associated effects rather than being attributed exclusively to the nanoparticles. Furthermore, although the supplied nanoparticles were characterized by the manufacturer, particle-size distributions, aggregation behavior, and suspension stability under the experimental preparation conditions were not independently evaluated. Consequently, the physicochemical state of the nanoparticle-based formulations at the time of application could not be fully established, limiting the reproducibility of their suspension properties and the interpretation of responses associated with specific nanoparticle characteristics.

5. Conclusions

Severe water limitation restricted biomass accumulation and fruit production in field-grown jalapeño pepper, while the evaluated foliar treatments induced distinct physiological, photochemical, and nutritional responses. The ZnO NP-based formulation showed the greatest capacity to sustain productive performance, maintaining fruit dry biomass at a level comparable to that of well-watered plants and substantially recovering aboveground biomass and fruit yield. In contrast, Codasil primarily enhanced photosynthetic and photochemical performance; Osmoplant maximized water-use efficiency; ZnO + SiO_2 NPs favored carboxylation efficiency; and Nano ZnMo contributed to maintaining a distinctive mineral nutrient profile. Correlation and PCA analyses further indicated associations between productivity and selected gas exchange and PSII photochemical traits, rather than establishing a uniform physiological response across treatments.

Finally, these findings highlight the differential benefits of the evaluated foliar formulations, with the ZnO NP-based formulation showing the greatest improvement in fruit productivity under water-limited conditions.

Author Contributions: The authors confirm their contribution to the paper as follows: study conception and design: E.H.O.-C. and E.S.; data collection: E.H.O.-C. and S.P.-Á.; analysis and interpretation of results: E.H.O.-C. and S.P.-Á.; draft manuscript preparation: E.H.O.-C. and E.S. All authors have read and agreed to the published version of the manuscript.

Funding: This research received no external funding.

Data Availability Statement: There is no additional associated data with this article. The data presented in this study are available on request from the corresponding author.

Acknowledgments: We would like to thank the Secretaría de Ciencia, Humanidades, Tecnología e Innovación (SECIHTI—Mexico) for the support provided by the scholarship granted to Erick Humberto Ochoa Chaparro through the "Becas Nacionales SECIHTI" program with CVU No. 843732.

Conflicts of Interest: The authors declare no conflicts of interest.

References

1. Tardieu, F.; Granier, C.; Muller, B. Water deficit and growth. Co-ordinating processes without an orchestrator? *Curr. Opin. Plant Biol.* **2011**, *14*, 283–289. [CrossRef] [PubMed]
2. Kang, J.; Peng, Y.; Xu, W. Crop Root Responses to Drought Stress: Molecular Mechanisms, Nutrient Regulations, and Interactions with Microorganisms in the Rhizosphere. *Int. J. Mol. Sci.* **2022**, *23*, 9310. [CrossRef] [PubMed]
3. Farooq, M.; Wahid, A.; Kobayashi, N.; Fujita, D.; Basra, S.M.A. Plant drought stress: Effects, mechanisms and management. *Agron. Sustain. Dev.* **2009**, *29*, 185–212. [CrossRef]

4. Seleiman, M.F.; Al-Suhaibani, N.; Ali, N.; Akmal, M.; Alotaibi, M.; Refay, Y.; Dindaroglu, T.; Abdul-Wajid, H.H.; Battaglia, M.L. Drought Stress Impacts on Plants and Different Approaches to Alleviate Its Adverse Effects. *Plants* **2021**, *10*, 259. [CrossRef] [PubMed]
5. Widuri, L.I.; Lakitan, B.; Sakagami, J.; Yabuta, S.; Kartika, K.; Siaga, E. Short-term drought exposure decelerated growth and photosynthetic activities in chili pepper (*Capsicum annuum* L.). *Ann. Agric. Sci.* **2020**, *65*, 149–158. [CrossRef]
6. Chaves, M.M.; Flexas, J.; Pinheiro, C. Photosynthesis under drought and salt stress: Regulation mechanisms from whole plant to cell. *Ann. Bot.* **2009**, *103*, 551–560. [CrossRef] [PubMed]
7. Flexas, J.; Bota, J.; Loreto, F.; Cornic, G.; Sharkey, T.D. Diffusive and metabolic limitations to photosynthesis under drought and salinity in C3 plants. *Plant Biol.* **2004**, *6*, 269–279. [CrossRef] [PubMed]
8. Baker, N.R. Chlorophyll fluorescence: A probe of photosynthesis in vivo. *Annu. Rev. Plant Biol.* **2008**, *59*, 89–113. [CrossRef] [PubMed]
9. Maxwell, K.; Johnson, G.N. Chlorophyll fluorescence—A practical guide. *J. Exp. Bot.* **2000**, *51*, 659–668. [CrossRef]
10. D'Oria, A.; Courbet, G.; Billiot, B.; Jing, L.; Pluchon, S.; Arkoun, M.; Maillard, A.; Paysant-Le Roux, C.; Trouverie, J.; Etienne, P.; et al. Drought specifically downregulates mineral nutrition: Plant ionomic content and associated gene expression. *Plant Direct* **2022**, *6*, e402. [CrossRef] [PubMed]
11. Hänsch, R.; Mendel, R.R. Physiological functions of mineral micronutrients (Cu, Zn, Mn, Fe, Ni, Mo, B, Cl). *Curr. Opin. Plant Biol.* **2009**, *12*, 259–266. [CrossRef] [PubMed]
12. Cakmak, I.; Brown, P.; Colmenero-Flores, J.M.; Husted, S.; Kutman, B.Y.; Nikolic, M.; Rengel, Z.; Schmidt, S.B.; Zhao, F.-J. Micronutrients. In *Marschner's Mineral Nutrition of Plants*, 4th ed.; Rengel, Z., Cakmak, I., White, P.J., Eds.; Academic Press: London, UK, 2023; pp. 283–385. [CrossRef]
13. Rasheed, A.; Li, H.; Tahir, M.M.; Mahmood, A.; Nawaz, M.; Shah, A.N.; Aslam, M.T.; Negm, S.; Moustafa, M.; Hassan, M.U.; et al. The role of nanoparticles in plant biochemical, physiological, and molecular responses under drought stress: A review. *Front. Plant Sci.* **2022**, *13*, 976179. [CrossRef] [PubMed]
14. Chandrashekar, H.K.; Singh, G.; Kaniyassery, A.; Thorat, S.A.; Nayak, R.; Murali, T.S.; Muthusamy, A. Nanoparticle-mediated amelioration of drought stress in plants: A systematic review. *3 Biotech* **2023**, *13*, 336. [CrossRef] [PubMed]
15. Karimian, Z.; Samiei, L. ZnO nanoparticles efficiently enhance drought tolerance in *Dracocephalum kotschyi* through altering physiological, biochemical and elemental contents. *Front. Plant Sci.* **2023**, *14*, 1063618. [CrossRef] [PubMed]
16. Haider, S.; Munyaneza, V.; Zhang, W.; Ren, L.; Song, H.; Ali, A.; Mehran, M.; Ahmad, I.A.; Kant, S.; Ding, G. Silicon dioxide nanoparticles improve drought tolerance in *Brassica napus* by modulating stomatal aperture via KAT1/AHA1 activation and photosynthetic carbon fixation. *Plant Physiol. Biochem.* **2025**, *229*, 110732. [CrossRef] [PubMed]
17. Dolatkhah Dashtmian, A.; Hosseini Mazinani, S.M.; Pazoki, A. Exogenous chitosan nanoparticles modulated drought stress through changing yield, biochemical attributes, and fatty acid profile of common bean (*Phaseolus vulgaris* L.) cultivars. *Gesunde Pflanz.* **2023**, *75*, 2463–2476. [CrossRef]
18. El-Ramady, H.; Sári, D.; Elsakhawy, T.; Abdalla, N.; Abd-Alla, H.I.; Prokisch, J. Nanotechnology for Drought Mitigation and Water Conservation: Opportunities and Limitations. *Nanomaterials* **2026**, *16*, 523. [CrossRef] [PubMed]
19. Mohammed, S.; Hussen, A. Influence of deficit irrigation levels on agronomic performance of pepper (*Capsicum annuum* L.) under drip at Alage, Central Rift Valley of Ethiopia. *PLoS ONE* **2023**, *18*, e0280639. [CrossRef] [PubMed]
20. Gil-Marín, J.A.; Zermeño-González, A.; Córdova-Rodríguez, M.X.; Ramírez-Rodríguez, H.; Cadena-Zapata, M.; Méndez-González, J.; Cornejo-Oviedo, E.H. Deficit irrigation on fruit yield and quality of sweet pepper. *Open Agric. J.* **2023**, *17*, e18743315273156. [CrossRef]
21. Haifa Group. NutriNet®: Precision Fertigation Recommendation Software. Available online: https://nutrinet.haifa-group.com/ (accessed on 10 January 2025).
22. Anchondo-Páez, J.C.; Sánchez-Chávez, E.; Ramirez-Estrada, C.A.; Salcido-Martínez, A.; Ochoa-Chaparro, E.H.; Muñoz-Márquez, E. Efficacy of silicon nanoparticles and Codasil® as potential biostimulants in green beans. *Terra Latinoam.* **2024**, *42*, e1885. [CrossRef]
23. Uddling, J.; Gelang-Alfredsson, J.; Piikki, K.; Pleijel, H. Evaluating the relationship between leaf chlorophyll concentration and SPAD-502 chlorophyll meter readings. *Photosynth. Res.* **2007**, *91*, 37–46. [CrossRef] [PubMed]
24. LI-COR Biosciences. *Using the LI-6400/LI-6400XT Portable Photosynthesis System: Instruction Manual*; Version 6; LI-COR Biosciences: Lincoln, NE, USA, 2011. Available online: https://www.baygenebiotech.com.cn/uploads/6f506bf154cdca0dab964f47402a6f06/download/Manual-LI-6400-v4-EN.pdf (accessed on 23 September 2026).
25. Farquhar, G.D.; Sharkey, T.D. Stomatal conductance and photosynthesis. *Annu. Rev. Plant Physiol.* **1982**, *33*, 317–345. [CrossRef]
26. Medrano, H.; Tomás, M.; Martorell, S.; Flexas, J.; Hernández, E.; Rosselló, J.; Pou, A.; Escalona, J.-M.; Bota, J. From leaf to whole-plant water use efficiency (WUE) in complex canopies: Limitations of leaf WUE as a selection target. *Crop J.* **2015**, *3*, 220–228. [CrossRef]

27. Wellburn, A.R. The spectral determination of chlorophylls *a* and *b*, as well as total carotenoids, using various solvents with spectrophotometers of different resolution. *J. Plant Physiol.* **1994**, *144*, 307–313. [CrossRef]
28. Irigoyen, J.J.; Einerich, D.W.; Sánchez-Díaz, M. Water stress induced changes in concentrations of proline and total soluble sugars in nodulated alfalfa (*Medicago sativa*) plants. *Physiol. Plant.* **1992**, *84*, 55–60. [CrossRef]
29. Ramírez-Estrada, C.A.; Sánchez, E.; Salcido-Martínez, A.; Anchondo-Páez, J.C.; Muñoz-Márquez, E.; Palacio-Márquez, A. Foliar nano Zn-Mo and chlorine dioxide affects use efficiency and distribution of macronutrients in green bean plants. *Plant Nano Biol.* **2025**, *11*, 100129. [CrossRef]
30. Cavell, A.J. The colorimetric determination of phosphorus in plant materials. *J. Sci. Food Agric.* **1955**, *6*, 479–480. [CrossRef]
31. Yan, S.; Weng, B.; Jing, L.; Bi, W. Effects of drought stress on water content and biomass distribution in summer maize (*Zea mays* L.). *Front. Plant Sci.* **2023**, *14*, 1118131. [CrossRef] [PubMed]
32. Ntanasi, T.; Karavidas, I.; Savvas, D.; Spyrou, G.P.; Giannothanasis, E.; Consentino, B.B.; Papasotiropoulos, V.; Sabatino, L.; Ntatsi, G. Physiological and yield responses of pepper (*Capsicum annuum* L.) genotypes to drought stress. *Plants* **2025**, *14*, 1934. [CrossRef] [PubMed]
33. Guzel Deger, A.; Çevik, S.; Kahraman, O.; Turunc, E.; Yakin, A.; Binzet, R. Effects of green and chemically synthesized ZnO nanoparticles on *Capsicum annuum* under drought stress. *Acta Physiol. Plant.* **2025**, *47*, 17. [CrossRef]
34. Shirvani-Naghani, S.; Fallah, S.; Pokhrel, L.R.; Rostamnejadi, A. Drought stress mitigation and improved yield in *Glycine max* through foliar application of zinc oxide nanoparticles. *Sci. Rep.* **2024**, *14*, 27898. [CrossRef] [PubMed]
35. Mushtaq, N.; Altaf, M.A.; Ning, J.; Shu, H.; Fu, H.; Lu, X.; Cheng, S.; Wang, Z. Silicon improves the drought tolerance in pepper plants through the induction of secondary metabolites, GA biosynthesis pathway, and suppression of chlorophyll degradation. *Plant Physiol. Biochem.* **2024**, *214*, 108919. [CrossRef] [PubMed]
36. Asargew, M.F.; Masutomi, Y.; Kobayashi, K.; Aono, M. Water stress changes the relationship between photosynthesis and stomatal conductance. *Sci. Total Environ.* **2024**, *907*, 167886. [CrossRef] [PubMed]
37. Padilla, Y.G.; Gisbert-Mullor, R.; López-Galarza, S.; Albacete, A.; Martínez-Melgarejo, P.A.; Calatayud, Á. Short-term water stress responses of grafted pepper plants are associated with changes in the hormonal balance. *Front. Plant Sci.* **2023**, *14*, 1170021. [CrossRef] [PubMed]
38. Almeida, E.C.; Pereira, F.H.F.; Ferreira, K.N.; de Sena Rodrigues, A.C.; Araújo, R.H.C.R.; de Souza, J.E.J.; Ramos, C.S.G.; Lopes, G.; dos Santos, L.C.; Neto, F.B.; et al. Physiological, Productive, and Nutritional Performance of Tomato Plants Treated with Iron and Zinc Nanoparticles via Foliar Application Under Deficit Irrigation. *Horticulturae* **2025**, *11*, 1228. [CrossRef]
39. Francesca, S.; Najai, S.; Zhou, R.; Decros, G.; Cassan, C.; Delmas, F.; Ottosen, C.-O.; Barone, A.; Rigano, M.M. Phenotyping to dissect the biostimulant action of a protein hydrolysate in tomato plants under combined abiotic stress. *Plant Physiol. Biochem.* **2022**, *179*, 32–43. [CrossRef] [PubMed]
40. Stefanov, M.; Rashkov, G.; Borisova, P.; Apostolova, E. Sensitivity of the Photosynthetic Apparatus in Maize and Sorghum under Different Drought Levels. *Plants* **2023**, *12*, 1863. [CrossRef] [PubMed]
41. Zahedi, S.M.; Hosseini, M.S.; Hoveizeh, N.F.; Kadkhodaei, S.; Vaculík, M. Comparative morphological, physiological and molecular analyses of drought-stressed strawberry plants affected by SiO_2 and SiO_2-NPs foliar spray. *Sci. Hortic.* **2023**, *309*, 111686. [CrossRef]
42. Mahmoud, A.W.M.; Rashad, H.M.; Esmail, S.E.A.; Alsamadany, H.; Abdeldaym, E.A. Application of Silicon, Zinc, and Zeolite Nanoparticles—A Tool to Enhance Drought Stress Tolerance in Coriander Plants for Better Growth Performance and Productivity. *Plants* **2023**, *12*, 2838. [CrossRef] [PubMed]
43. Liu, C.; Sun, H.; Xu, Y.; Wu, C. Effects of SiO_2 nanoparticles on root structures, gas exchange, and antioxidant activities of *Cunninghamia lanceolata* seedlings under drought stress. *J. Plant Nutr.* **2023**, *46*, 3771–3793. [CrossRef]
44. Trejo-Paniagua, B.O.; Caamal-Chan, M.G.; Cruz-Rodríguez, R.I.; Lam-Gutiérrez, A.; Ruiz-Lau, N. Physiological, Biochemical, and Molecular Response in Siete Caldos Chili Pepper Plants (*Capsicum frutescens*) Exposed to Water Deficit. *Horticulturae* **2024**, *10*, 558. [CrossRef]
45. Nikzad, S.; Sharafi, S.; Hamze, H.; Mahmoodi, T.M.; Yazdan Seta, S. Investigating the effect of foliar spraying of zinc nanoparticles and biostimulants on modulating the effect of water deficit stress in sugar beet by using Integrated Biomarker Response Version 2. *Sci. Rep.* **2025**, *15*, 37780. [CrossRef] [PubMed]
46. Iqbal, B.; Hussain, F.; Khan, M.S.; Iqbal, T.; Shah, W.; Ali, B.; Al Syaad, K.M.; Ercisli, S. Physiology of gamma-aminobutyric acid treated *Capsicum annuum* L. (Sweet pepper) under induced drought stress. *PLoS ONE* **2023**, *18*, e0289900. [CrossRef] [PubMed]
47. Mendoza-Alatorre, M.; Infante-Ramírez, R.; González-Rangel, M.O.; Nevárez-Moorillón, G.V.; González-Horta, M.C.; Hernández-Huerta, J.; Delgado-Gardea, M.C.E. Enhancing drought stress tolerance and growth promotion in chiltepin pepper (*Capsicum annuum* var. *glabriusculum*) through native *Bacillus* spp. *Sci. Rep.* **2024**, *14*, 15383. [CrossRef] [PubMed]
48. Bitik, S.K.; Aydemir, Ö.E.; Kocaman, A.; Turan, M.; Özkutlu, F. Physiological and biochemical ameliorative effects of biochar, *Trichoderma harzianum*, and combined applications in *Capsicum annuum* L. under water stress. *Plant Growth Regul.* **2026**, *106*, 3. [CrossRef]

49. Maphalaphathwa, M.; Nciizah, A.D. Nutrient Seed Priming Effects on Water Stress Tolerance and Nutrient Uptake of Chilies (*Capsicum annum* L.). *Agronomy* **2025**, *15*, 930. [CrossRef]
50. Martins, B.L.R.; Ferreira, K.N.; Rocha, J.L.A.; Araujo, R.H.C.R.; Lopes, G.; Santos, L.C.d.; Bezerra Neto, F.; Sá, F.V.d.S.; Silva, T.I.d.; da Silva, W.I.; et al. Nano ZnO and Bioinoculants Mitigate Effects of Deficit Irrigation on Nutritional Quality of Green Peppers. *Horticulturae* **2024**, *10*, 969. [CrossRef]
51. Al-Selwey, W.A.; Alsadon, A.A.; Alenazi, M.M.; Tarroum, M.; Ibrahim, A.A.; Ahmad, A.; Osman, M.; Seleiman, M.F. Morphological and Biochemical Response of *Potatoes* to Exogenous Application of ZnO and SiO_2 Nanoparticles in a Water Deficit Environment. *Horticulturae* **2023**, *9*, 883. [CrossRef]
52. Melo-Sabogal, D.V.; Guevara-Gonzalez, R.G.; Torres-Pacheco, I.; Millan-Almaraz, J.R.; Guzmán-Cruz, R.; Contreras-Medina, L.M. β values obtained by linear regression models of morpho-physiological and biochemical variables as novel drought stress estimators in *Capsicum annuum* varieties. *Plant Stress* **2024**, *14*, 100588. [CrossRef]
53. Camoglu, G.; Demirel, K.; Kahriman, F.; Akcal, A.; Nar, H. Plant-based monitoring techniques to detect yield and physiological responses in water-stressed pepper. *Agric. Water Manag.* **2024**, *291*, 108628. [CrossRef]
54. Raza, M.A.S.; Amin, J.; Valipour, M.; Iqbal, R.; Aslam, M.U.; Zulfiqar, B.; Muhammad, F.; Ibrahim, M.A.; Al-Ghamdi, A.A.; Elshikh, M.S.; et al. Cu-nanoparticles enhance the sustainable growth and yield of drought-subjected wheat through physiological progress. *Sci. Rep.* **2024**, *14*, 14254. [CrossRef] [PubMed]
55. Liang, X.; Liao, Q.; Guo, P.; Yang, Z.; Kang, S.; Du, T.; Tong, L.; Ding, R. Silicon nanoparticles enhance maize yield and water productivity via regulating photosynthesis and canopy structure under mild regulated deficit irrigation. *Front. Plant Sci.* **2025**, *16*, 1691443. [CrossRef] [PubMed]

Disclaimer/Publisher's Note: The statements, opinions and data contained in all publications are solely those of the individual author(s) and contributor(s) and not of MDPI and/or the editor(s). MDPI and/or the editor(s) disclaim responsibility for any injury to people or property resulting from any ideas, methods, instructions or products referred to in the content.